USGS
science for a changing world

Prepared in cooperation with the New York City Department of Environmental Protection

Bathymetry of New York City’s East of Hudson Reservoirs and Controlled Lakes, 2017 to 2019

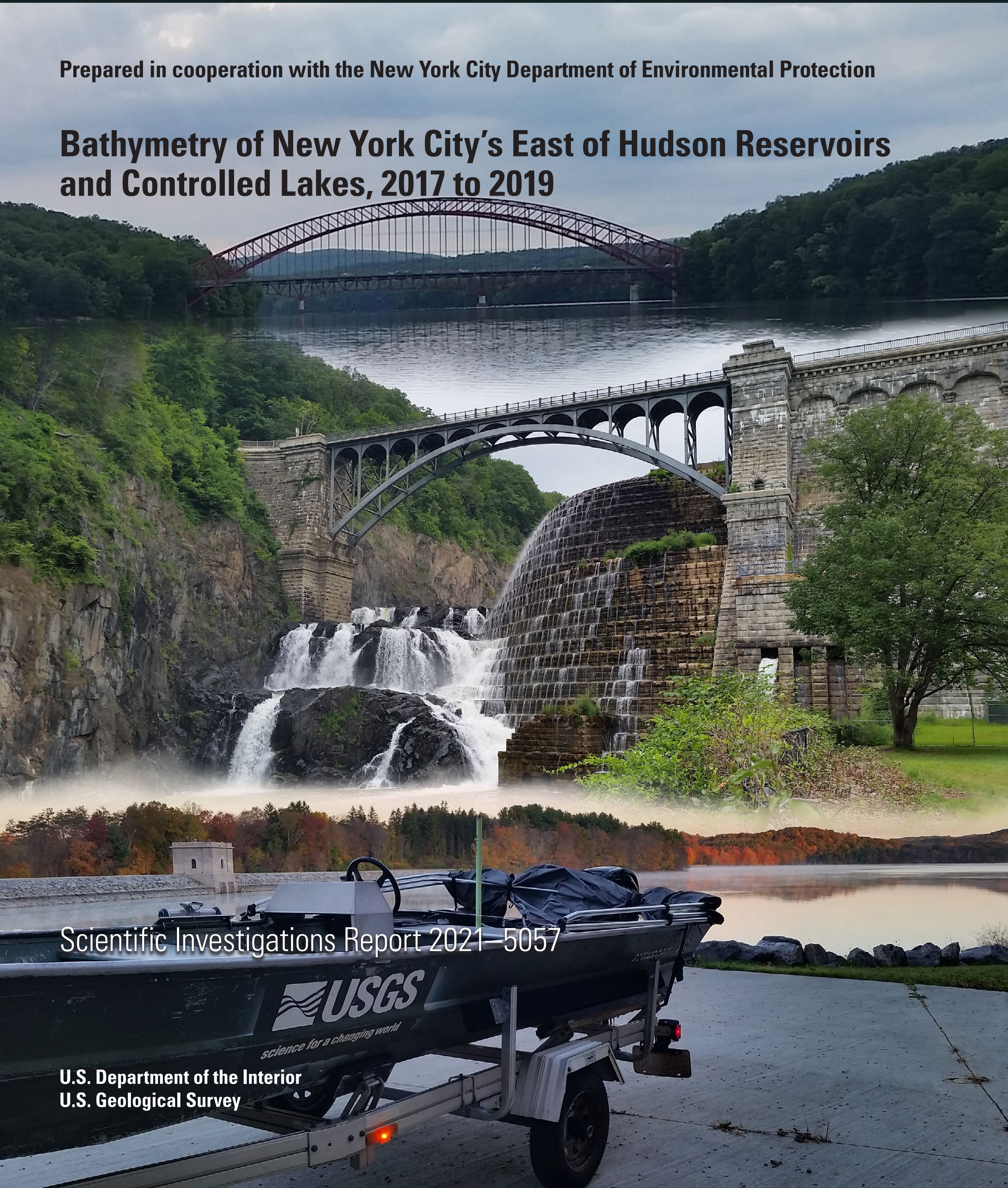

Scientific Investigations Report 2021–5057

U.S. Department of the Interior
U.S. Geological Survey

Front cover. [top] A bridge on the Taconic Parkway over New Croton Reservoir, New York. [middle] The dam and spillway at New Croton Reservoir. [bottom] A U.S. Geological Survey boat at Bog Brook Reservoir. Photographs by Elizabeth Nystrom, U.S. Geological Survey.

Back cover. New Croton Reservoir in New York; photograph by Elizabeth Nystrom, U.S. Geological Survey.

Bathymetry of New York City's East of Hudson Reservoirs and Controlled Lakes, 2017 to 2019

By Elizabeth A. Nystrom, Courtney J. Huston, and Robert J. Welk

Prepared in cooperation with the
New York City Department of Environmental Protection

Scientific Investigations Report 2021–5057

U.S. Department of the Interior
U.S. Geological Survey

U.S. Geological Survey, Reston, Virginia: 2021

For more information on the USGS—the Federal source for science about the Earth, its natural and living resources, natural hazards, and the environment—visit https://www.usgs.gov or call 1–888–ASK–USGS.

For an overview of USGS information products, including maps, imagery, and publications, visit https://store.usgs.gov/.

Suggested citation:
Nystrom, E.A., Huston, C.J., and Welk, R.J., 2021, Bathymetry of New York City's East of Hudson reservoirs and controlled lakes, 2017 to 2019: U.S. Geological Survey Scientific Investigations Report 2021–5057, 46 p., https://doi.org/10.3133/sir20215057.

Data associated with this publication:
Nystrom, E.A., Huston, C.J., and Welk, R.J., 2021, Geospatial bathymetry datasets for New York City's East of Hudson reservoirs and controlled lakes: U.S. Geological Survey data release, https://doi.org/10.5066/P9ZZQ2OT.

ISSN 2328-0328 (online)

Acknowledgments

The authors would like to thank the New York City Department of Environmental Protection, notably, Jordan Gass and Adolf Jonietz, for providing practical information about the reservoirs and local datums and additional survey data for quality assurance use, Lori DiLorenzo for coordinating reservoir access, and Michael Ansaldi and the boat office crew for steam cleaning the boat many times. The authors would also like to thank Meaghan Keefe and Todd Campbell of the U.S. Geological Survey for their immense help in collecting the data used in this report.

Contents

Figures

Tables

Conversion Factors

U.S. customary units to International System of Units

Multiply	By	To obtain
foot (ft)	0.3048	meter (m)
mile (mi)	1.609	kilometer (km)
acre	0.4047	hectare (ha)
square mile (mi^2)	2.590	square kilometer (km^2)
gallon (gal)	3.785	liter (L)
million gallons (Mgal)	3,785	cubic meter (m^3)
acre-foot (ac-ft)	1,233	cubic meter (m^3)

Temperature in degrees Celsius (°C) may be converted to degrees Fahrenheit (°F) as follows:

$$°F = (1.8 \times °C) + 32.$$

Temperature in degrees Fahrenheit (°F) may be converted to degrees Celsius (°C) as follows:

$$°C = (°F – 32) / 1.8.$$

Datums

Vertical coordinate information is referenced to the North American Vertical Datum of 1988 (NAVD 88).

Horizontal coordinate information is referenced to the North American Datum of 1983 (NAD 83).

Elevation, as used in this report, refers to distance above the vertical datum.

Abbreviations

ADCP	acoustic Doppler current profiler
EOH	East of Hudson
GIS	geographic information system
GNSS	global navigation satellite system
INS	inertial navigation system
lidar	light detection and ranging
NSSDA	National Standard for Spatial Data Accuracy
NYCDEP	New York City Department of Environmental Protection
POS MV	Position Orientation Solution for Marine Vessels
RTK	real-time kinematic
RMSE	root mean square error
TIN	triangulated irregular network
USGS	U.S. Geological Survey
VRS	virtual reference station network
WOH	West of Hudson

Bathymetry of New York City's East of Hudson Reservoirs and Controlled Lakes, 2017 to 2019

By Elizabeth A. Nystrom, Courtney J. Huston, and Robert J. Welk

Abstract

New York City maintains an extensive system of reservoirs and aqueducts to provide drinking water to its residents, including 16 reservoirs and controlled lakes in Westchester and Putnam Counties in southern New York, east of the Hudson River (also called "East of Hudson reservoirs and controlled lakes"). These reservoirs were put into service from 1842 to 1915, and their capacities have likely changed since their original construction. To provide updated bathymetric surface, contour, and capacity data, the U.S. Geological Survey, in cooperation with New York City Department of Environmental Protection, surveyed the bathymetry of the 16 East of Hudson reservoirs and controlled lakes from 2017 to 2019 using a multibeam echosounder. The points measured with the multibeam echosounder were combined with light detection and ranging data to generate 3.28-foot raster grids of the bathymetric surfaces, bathymetric contours at 2-foot intervals of elevation, and elevation-area-capacity tables. The results of the bathymetric survey show that the East of Hudson reservoirs range from about 25 feet deep (Kirk Lake) to about 162 feet deep (Kensico Reservoir) and have a total capacity of 142.9 billion gallons, with a combined surface area of more than 11,600 acres.

The accuracy of the mapped bathymetric data was evaluated using quality assurance datasets collected with a single-beam echosounder; about 284,000 quality assurance points were spatially joined with the mapped raster surface to compute measurement errors. The calculated mean point elevation error for the East of Hudson reservoirs was 0.35 foot, the median error was 0.21 foot, and the 95-percent accuracy was 1.68 feet; the 95-percent accuracy of the computed capacity at spillway elevation was 1.6 percent or less. The largest errors occurred in the steepest areas of the reservoirs and in areas where the data were interpolated. Geospatial files of the bathymetry data, including mapped bathymetric surfaces, contours, and capacity tables, quality assurance points, and associated metadata are available for download as part of an accompanying U.S. Geological Survey data release.

Introduction

The New York City Department of Environmental Protection (NYCDEP) maintains an extensive system of reservoirs and aqueducts for water collection, storage, and transport; the City provides more than 1 billion gallons of drinking water to more than 9 million people every day (NYCDEP, 2020b). New York City maintains and uses 13 reservoirs and 3 lakes in Putnam and Westchester Counties in southern New York, east of the Hudson River (known as "East of Hudson [or EOH] reservoirs and controlled lakes"). The NYCDEP depends on bathymetric data for the daily and seasonal management of the EOH reservoirs and controlled lakes; these data include the mapped bathymetric surfaces and contours of the lakes and reservoirs and computed elevation-area-capacity tables. The bathymetric surfaces and contours are used in water-quality models and mapping applications, and the elevation-area-capacity tables are used to determine current and available reservoir storage. The bathymetry of the EOH reservoirs was initially determined from the land surface before each reservoir was built; the newest EOH reservoir was placed into service more than 100 years ago (NYCDEP, 2021h), and since their initial filling, the capacity and bed morphology of the reservoirs is likely to have changed. To provide updated surface, contour, and capacity data, the U.S. Geological Survey (USGS), in cooperation with NYCDEP, surveyed the bathymetry of the 16 EOH reservoirs and controlled lakes from 2017 to 2019. The accuracy of the mapped bathymetric data was evaluated using quality assurance datasets collected with a single-beam echosounder; about 284,000 quality assurance points were spatially joined with the mapped raster surfaces to compute measurement errors.

Purpose and Scope

The purpose of this report is to document bathymetric survey results for New York City's 16 East of Hudson reservoirs and controlled lakes completed from May 2017 to November 2019 using a multibeam echosounder. Equipment and methods of data collection and processing are described and results, including a data accuracy assessment, are presented.

Description of Study Area

New York City's East of Hudson reservoirs and controlled lakes (fig. 1; table 1) are in the Croton and Bronx River basins in Putnam and Westchester Counties in southern New York State, about 15 to 40 miles north of the City; the EOH reservoirs and controlled lakes form New York City's Croton Water Supply System and also include designated parts of the Catskill and Delaware Water Supply Systems. Construction of the EOH reservoirs began in 1837 at Croton Reservoir; water from Croton Reservoir was first delivered to the city in 1842 (NYCDEP, 2020a). The Croton Water Supply System was expanded with the construction of several additional reservoirs in the late 1800s (table 1), and the original Croton Reservoir was replaced with the combination of New Croton and Muscoot Reservoirs, which were placed into service in 1905 (NYCDEP, 2021j, k). The newest EOH reservoir, Kensico Reservoir, was placed into service in 1915 (NYCDEP, 2021h).

Three controlled lakes are also part of the Croton Water Supply System: Lake Gilead, Lake Gleneida, and Kirk Lake (table 1); these are lakes that the NYCDEP either owns or has the rights to withdraw water from. The Catskill and Delaware Water Supply Systems were constructed beginning in the early 1900s and contain New York City's six West of Hudson (WOH) reservoirs (not included in this report): Ashokan and Schoharie Reservoirs in the Catskill Water Supply System, and Cannonsville, Neversink, Pepacton, and Rondout Reservoirs in the Delaware Water Supply System. Aqueducts connect the WOH reservoirs to the EOH reservoirs, and as a result, three of the EOH reservoirs—Boyd Corners (NYCDEP, 2021c), Kensico (NYCDEP, 2021h), and West Branch Reservoirs (NYCDEP, 2021m)—are part of the Catskill and Delaware Water Supply Systems (table 1). The WOH reservoirs were mapped with a single-beam echosounder as part of a separate bathymetric survey from 2013 to 2015 (Nystrom, 2018).

Table 1. New York City's East of Hudson reservoirs and controlled lakes, in Westchester and Putnam Counties, New York.

[Locations of reservoirs shown on figure 1. —, not applicable]

Reservoir	Type of waterbody	Year placed into service[1]	Water supply system
Amawalk Reservoir	Reservoir	1897	Croton
Bog Brook Reservoir	Reservoir	1892	Croton
Boyd Corners Reservoir	Reservoir	1873	Delaware
Cross River Reservoir	Reservoir	1908	Croton
Croton Falls Reservoir	Reservoir	1911	Croton
Diverting Reservoir	Reservoir	1911	Croton
East Branch Reservoir	Reservoir	1891	Croton
Lake Gilead	Controlled lake	—	Croton
Lake Gleneida	Controlled lake	—	Croton
Kensico Reservoir	Reservoir	1915	Catskill and Delaware
Kirk Lake	Controlled lake	—	Croton
Middle Branch Reservoir	Reservoir	1878	Croton
Muscoot Reservoir	Reservoir	1905	Croton
New Croton Reservoir[2]	Reservoir	1905	Croton
Titicus Reservoir	Reservoir	1893	Croton
West Branch Reservoir	Reservoir	1895	Delaware

[1]Data are from New York City Department of Environmental Protection (NYCDEP, 2021a-m).

[2]The New Croton Reservoir is an enlargement of the Croton Reservoir, which had been placed into service in 1842 (NYCDEP, 2021k).

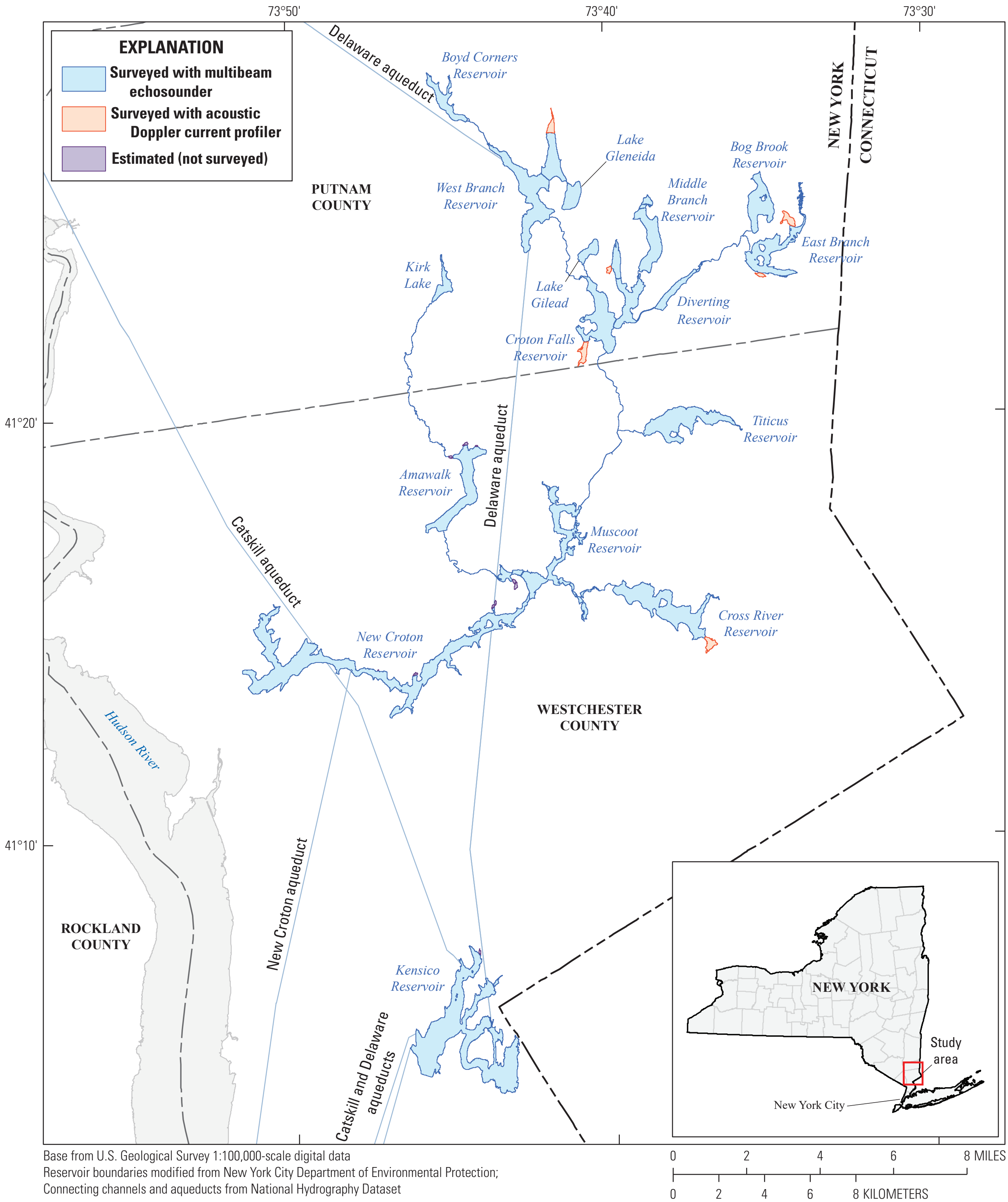

Figure 1. Map showing locations of New York City's East of Hudson reservoirs and controlled lakes, connecting channels, and aqueducts, in Westchester and Putnam Counties, New York.

Data Collection and Processing Methods

Bathymetry in the 16 EOH reservoirs and controlled lakes was surveyed from May 2017 to November 2019 (table 2). Data were primarily collected using a multibeam echosounder deployed from a moving boat (fig. 2). Some small areas (fig. 1) that were inaccessible with the boat used to deploy the multibeam echosounder (which required a trailer) were surveyed with an acoustic Doppler current profiler (ADCP). Quality assurance data were collected using a single-beam echosounder and compared with the multibeam echosounder dataset. Ancillary data were measured and used in processing the echosounder data and included the water surface elevation at each reservoir (for vertical position data) and sound velocity profiles. Vertical coordinate information is referenced to the North American Vertical Datum of 1988 (NAVD 88) using GEOID09. Horizontal coordinate information is referenced to the North American Datum of 1983 (NAD 83).

Table 2. Dates and method used to survey bathymetry in New York City's East of Hudson reservoirs, in Westchester and Putnam Counties, New York.

[Locations of reservoirs shown on figure 1. Survey data are available in Nystrom and others (2021). ADCP, acoustic Doppler current profiler; —, not applicable]

Reservoir	Multibeam survey date	Single-beam survey date	ADCP survey date
Amawalk Reservoir	5/16/2018–5/18/2018, 5/21/2018, 11/04/2019–11/06/2019	5/21/2018	—
Bog Brook Reservoir	10/27/2017, 10/31/2017	10/31/2017	—
Boyd Corners Reservoir	9/27/2017–9/28/2017	9/28/2017	—
Cross River Reservoir	6/19/2018–6/21/2018, 6/25/2018–6/27/2018	6/21/2018	10/21/2019
Croton Falls Reservoir	8/29/2017–8/31/2017, 5/14/2018	8/30/2017–8/31/2017, 5/14/2018	10/23/2019–10/24/2019
Diverting Reservoir	6/26/2017–6/28/2017	6/27/2017	—
East Branch Reservoir	5/23/2018–5/25/2018, 6/18/2018	6/18/2018	10/23/2019
Lake Gilead	5/22/2017–5/23/2017	5/23/2017	—
Lake Gleneida	5/24/2017	5/25/2017	—
Kensico Reservoir	6/27/2018, 6/29/2018, 7/17/2018–7/20/2018, 7/26/2018, 8/20/2018–8/23/2018	7/26/2018, 8/24/2018	—
Kirk Lake	6/22/2017	6/23/2017	—
Middle Branch Reservoir	7/28/2017, 8/2/2017–8/3/2017	8/3/2017	—
Muscoot Reservoir	6/5/2017–6/9/2017, 6/20/2017, 11/6/2019–11/7/2019	6/21/2017	—
New Croton Reservoir	6/28/2017, 7/19/2017–7/21/2017, 7/24/2017–7/26/2017, 10/26/2017	7/27/2017	—
Titicus Reservoir	11/2/2017–11/3/2017, 5/15/2018, 5/22/2018	5/22/2018	—
West Branch Reservoir	9/18/2017–9/21/2017, 9/26/2017, 10/25/2017	9/25/2017, 10/25/2017	10/22/2019

Figure 2. Photograph of survey boat and global navigation satellite system (GNSS) receivers used for the bathymetric surveys of New York City's East of Hudson reservoirs, in Westchester and Putnam Counties, New York; photograph by Elizabeth Nystrom, U.S. Geological Survey.

Vertical Control and Water Surface Elevation

Vertical control was established at each reservoir during the bathymetric surveys using global navigation satellite system (GNSS) surveys to determine water surface elevations referenced to NAVD 88 (table 3) using a survey-grade Trimble Inc. R8 receiver (fig. 3; Trimble Inc., 2009), with a mix of static observations and real-time kinematic (RTK) observations. Static observations were postprocessed in Trimble Business Center version 5.20 (Trimble Inc., 2021); RTK observations were made using the continuously operating virtual reference station (VRS) network NYSNet operated by the New York State Department of Transportation (2021). Data about each individual GNSS observation of water surface elevations, including dilution of precision values and epochs observed, are available in Nystrom and others (2021).

Time series of water surface elevations were used to convert measured bathymetric depths to elevations referenced to NAVD 88; water surface elevation time series are available in Nystrom and others (2021). For the majority of the surveys, an unvented pressure transducer was installed in shallow water, typically near the boat ramp, on a metal post pounded solidly into the sediment (fig. 4); a second pressure transducer was installed nearby above the water surface to measure barometric pressure. A time series of the depth of the water column above the pressure transducer (corrected for water temperature and barometric pressure) was calculated for each reservoir; a time series of water surface elevation referenced to NAVD 88 was then computed using the GNSS observations of water surface elevation. A limited number of surveys were done over a short time (a few hours or less), during which the water surface elevation did not change. A constant time series of water surface elevation was generated for these surveys using the average of the GNSS observations of water surface elevation; these surveys included the ADCP surveys of small areas of Cross River, Croton Falls, East Branch, and West Branch Reservoirs and single-day, multibeam surveys of parts of West Branch Reservoir (October 25, 2017), New Croton Reservoir (October 26, 2017), and Croton Falls Reservoir (May 14, 2018).

Sound Velocity

Echosounders measure depth by transmitting a pulse of sound into the water and measuring the amount of time it takes for an echo to return; to accurately calculate depth, the sound velocity must be known. Sound velocity varies with temperature, pressure, and salinity; reservoirs are often stratified by temperature, so the sound velocity usually varies with depth. Additionally, sound velocity profiles over depth can vary by location because water in shallow areas may warm differently than in deep areas. To account for the change of sound velocity

Table 3. Summary of global navigation satellite system observations of water surface elevations at New York City's East of Hudson reservoirs and controlled lakes, in Westchester and Putnam Counties, New York.

[Locations of reservoirs shown on figure 1. Survey data are available in Nystrom and others (2021). RTK, real-time kinematic; hh:mm:ss, hour, minute, second; —, not applicable]

Reservoir	Number of RTK observations	Total RTK epochs observed	Number of static observations	Total duration of static observations, in hh:mm:ss
Amawalk Reservoir	13	5,136	7	10:42:25
Bog Brook Reservoir	3	3,040	0	—
Boyd Corners Reservoir	4	2,363	0	—
Cross River Reservoir	14	2,519	9	2:31:52
Croton Falls Reservoir	8	4,946	1	1:32:00
Diverting Reservoir	4	1,132	0	—
East Branch Reservoir	8	7,703	3	4:11:04
Lake Gilead	2	1,410	0	—
Lake Gleneida	3	1,120	0	—
Kensico Reservoir	24	15,868	4	11:46:39
Kirk Lake	4	1,161	0	—
Middle Branch Reservoir	5	1,868	0	—
Muscoot Reservoir	13	4,022	6	3:24:10
New Croton Reservoir	16	5,269	0	—
Titicus Reservoir	8	3,171	3	9:54:17
West Branch Reservoir	15	7,778	1	2:17:44
Total	144	68,506	34	46:20:11

Figure 3. Photograph of global navigation satellite system (GNSS) rover receiver used to measure water surface elevation, referenced to North American Vertical Datum of 1988 (NAVD 88), on October 27, 2017, at Bog Brook Reservoir in Putnam County, New York; photograph by Elizabeth Nystrom, U.S. Geological Survey.

Figure 4. Photograph of installation of pressure transducer used to measure water surface elevation on May 23, 2017, at Lake Gilead in Putnam County, New York; photograph by Elizabeth Nystrom, U.S. Geological Survey.

over depth and area, profiles were measured at various locations at each lake or reservoir using an AML Oceanographic Smart SV sensor (AML Oceanographic, 2010).

Sound velocity profiles were measured at least once per day, and usually several times during each day, especially when data were collected in different areas of a reservoir (for example, shallow inlet bays and deep areas near dams). Sound velocity was recorded at 5-foot (ft) increments from the surface to the deepest depth possible at the location of measurement; the full depth at each location was measured unless the depth exceeded the length of the cable attached to the sound velocity probe (about 150 ft) or under very windy conditions that did not allow the cable of the sound velocity probe to hang vertically in the water. The cable was marked to indicate the depth of the probe, so if the cable was not vertical, the indicated depth would be higher than the actual depth of the probe. In breezy conditions, the boat motor was used to hold the position of the boat in place so the sound velocity probe cable could remain vertical. As a quality assurance check, water temperature at the reservoir surface was also measured with a thermistor during each sound velocity profile. A total of 235 individual sound velocity profiles were measured during the survey of the East of Hudson reservoirs (table 4). These individual measured sound velocity profiles were plotted and visually examined (fig. 5); where similar, profiles were grouped by date and location within a reservoir to generate average profiles for the reservoir. A total of 58 average profiles were computed for application to echosounder data (table 5). The measured and averaged sound velocity profiles used are available in Nystrom and others (2021).

Multibeam Echosounder

A multibeam echosounder uses sound to measure water depths at many locations simultaneously along a line (also called a swath) perpendicular to the echosounder. Multibeam echosounders are manufactured in many configurations, but they often use two phased-array transducers to shape acoustic transmit and receive beams and slice the acoustic returns into hundreds of individual depth measurements along each swath. To accurately map the depth measurements in space, multibeam echosounders are used with an inertial navigation system (INS) to measure the heave, pitch, roll, heading, and position of the echosounder. Multibeam echosounders and examples of their use for surveying rivers and lakes are described in Huizinga (2016) and Huizinga and Heimann (2018).

Table 4. Summary of sound velocity profiles measured in New York City's East of Hudson reservoirs, in Westchester and Putnam Counties, New York.

[Locations of reservoirs shown on figure 1. Survey data are available in Nystrom and others (2021)]

Reservoir	Number of sound velocity profiles	Number of groups of averaged profiles of sound velocity
Amawalk Reservoir	15	2
Bog Brook Reservoir	6	2
Boyd Corners Reservoir	6	1
Cross River Reservoir	18	3
Croton Falls Reservoir	13	5
Diverting Reservoir	7	2
East Branch Reservoir	14	4
Lake Gilead	4	1
Lake Gleneida	3	1
Kensico Reservoir	52	19
Kirk Lake	8	1
Middle Branch Reservoir	11	1
Muscoot Reservoir	25	5
New Croton Reservoir	23	4
Titicus Reservoir	8	3
West Branch Reservoir	22	4
Total	235	58

Multibeam Echosounder Data Collection

Bathymetric data were collected with a Teledyne MB2 multibeam echosounder (fig. 6; Teledyne Marine Odom Hydrographic, 2021) with an integrated Applanix Position Orientation Solution for Marine Vessels (POS MV) Wavemaster II INS (Applanix Corp., 2017) and an integrated Teledyne SVP 70 sound velocity sensor (Teledyne RESON, 2021). The MB2 has up to 256 adjustable-frequency beams—from 200 to 460 kilohertz (kHz)—with up to a 140-degree (°) swath width and configurable beam width (nominal beam width 1.8°). The multibeam echosounder data were collected from a flat-bottomed (jon) boat (fig. 2), between May 22, 2017, and November 7, 2019 (table 2). Primary multibeam data were collected during 2017 and 2018, but Amawalk and Muscoot Reservoirs were revisited in late 2019 to collect additional data.

The MB2 echosounder data were displayed and recorded using Teledyne PDS software (Teledyne PDS, 2019, 2021a, b) version 4.1.5.3 in 2017 and version 4.3.0.1 in 2018 and 2019. PDS creates a raster grid of raw measured depths in real time; this raster grid was used by the boat driver to navigate for the most complete coverage of the bathymetric surface possible. Data from adjacent MB2 measurement swaths were generally spaced to overlap at the edges by 10 to 25 percent; these overlapping areas were used as an additional quality assurance check during processing to verify reproducibility of point measurements after correcting for pitch, roll, heading, and sound velocity. The MB2 was generally operated at 460 kHz with 256 beams and 140° swath width, but in some areas, changes to the configuration of the MB2 were made because of field conditions. For example, in areas of excessive aquatic plant growth, the frequency of the MB2 was lowered to 200 kHz for a stronger reflection from the bottom of the reservoir. The minimum depth measurable with the MB2 was approximately 2 ft, and the maximum depth recorded by the MB2 was about 162 ft, at Kensico Reservoir. Some areas with especially dense aquatic weeds could not be measured with the MB2 because an acoustic return from the reservoir bottom could not be detected and the vegetation obstructed the sound velocity sensor. The mapping process for these areas is described in the "Bathymetric Map Creation" section of this report.

The position data from the Wavemaster II INS was supplemented with GNSS position data from a Trimble Inc. R8 GNSS receiver positioned directly above the echosounder transducer. The R8 GNSS receiver was operated in real-time kinematic mode via the NYSNet VRS over cellular modem whenever possible; some data were recorded in stand-alone or differential GNSS mode, typically because of poor cellular data reception. Position and depth data were synchronized using the $GPZDA string output by the R8 receiver. The $GPZDA string, which logs the Coordinated Universal Time (UTC) date and time, is defined by the National Marine Electronics Association 0183 standard (NMEA 0183) and contains a time stamp associated with a pulse-per-second signal (National Marine Electronics Association, 2002). In cases where RTK GNSS from the R8 receiver was not available or not consistently available (for example, due to poor cellular data connection) the position and depth data were not synchronized in the field. These data were processed after collection (postprocessing) to estimate a latency duration (within a few tenths of a second) to shift position data to match depth data. High grid-cell standard deviation values (available as geospatial data in Nystrom and others, 2021) reflect these poor synchronization conditions for areas measured with more than one pass of multibeam echosounder data (for example, in the large bay on the northern side of New Croton Reservoir near the spillway).

Multibeam Echosounder Data Processing

The multibeam echosounder data were processed using PDS version 4.3.7.5 (Teledyne PDS, 2021a, b). Multibeam echosounder processing included correction for changes in sound velocity over depth, conversion from depth to elevation above NAVD 88, application of INS calibration values, and editing to remove erroneous points or spikes.

The individually measured sound velocity profiles were averaged to form group profiles for correction of the multibeam echosounder data ("Sound Velocity" section of this report; table 5). The corrections of the multibeam echosounder

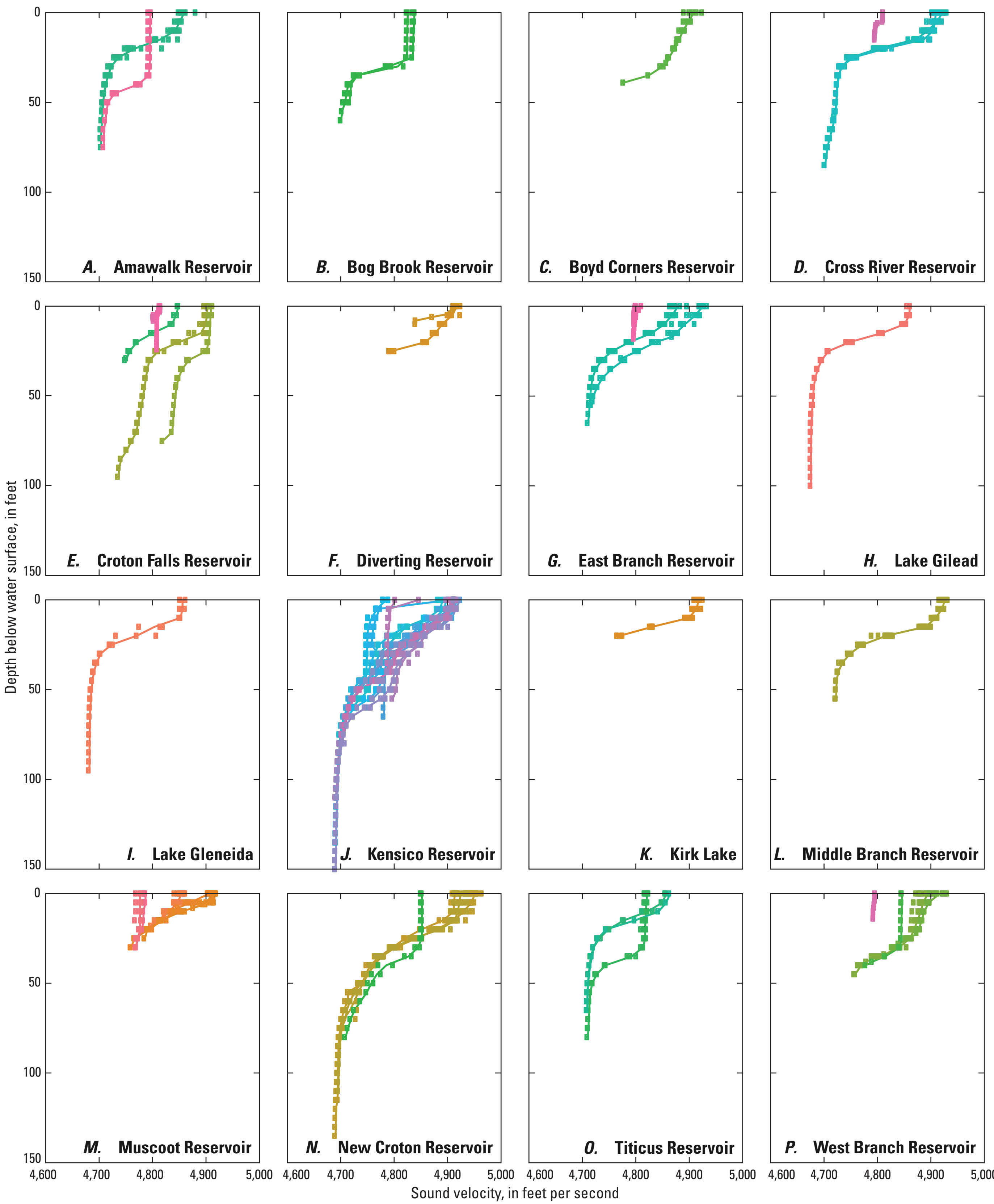

Figure 5. Graphs showing sound velocity profiles for New York City's East of Hudson reservoirs and controlled lakes, in Westchester and Putnam Counties, New York.

EXPLANATION

Sound velocity, average group profile—Circles (data points) are individual observations; lines are average profiles. Profile groups listed in table 5 of this report

20170522_23_Gilead
20170524_25_Gleneida
20170605_09_Muscoot
20170620_21_Muscoot_Bay
20170620_21_Muscoot_Narrow
20170622_23_Kirk
20170626_27_Diverting
20170627_Inlet_Diverting
20170628_NewCroton
20170719_21_NewCroton
20170724_27_NewCroton
20170728_0803_MiddleBranch
20170829_30_CrotonFalls_WestBasin
20170831_CrotonFalls_EastBasin
20170918_25_WestBranch_WestBasin
20170925_26_WestBranch_EastBasin
20170927_28_Boyd
20171025_WestBranch_WestBasin
20171026_NewCroton
20171027_BogBrook
20171031_BogBrook
20171102_03_Titicus
20180514_CrotonFalls_NorthBasin
20180515_Titicus
20180516_21_Amawalk
20180522_Titicus
20180523_25_EastBranch
20180618_EastBranch
20180619_21_CrossRiver
20180625_27_CrossRiver
20180627_29_Kensico_MainBay
20180627_29_Kensico_Ring
20180627_Kensico_Delaware
20180717_20_Kensico_MainBay
20180718_19_Kensico_Delaware
20180718_19_Kensico_DelawareOutlet
20180718_19_Kensico_Ring
20180720_Kensico_NorthArm
20180726_Kensico_MainBay
20180726_Kensico_Middle
20180726_Kensico_Ring
20180820_24_Kensico_MainBay
20180820_24_Kensico_Middle
20180820_24_Kensico_Rye
20180822_24_Kensico_NorthArm
20180824_Kensico_Delaware_Mid
20180824_Kensico_Delaware_N
20180824_Kensico_Delaware_South
20180824_Kensico_Ring
20191021_CrossRiver_EastCutoff
20191022_WestBranch_Cutoff
20191023_CrotonFalls_NorthBasinWestCutoff
20191023_EastBranch_NorthCutoff
20191023_EastBranch_SouthCutoff
20191024_CrotonFalls_SouthCutoff
20191104_06_Amawalk
20191106_Muscoot
20191107_Muscoot

Figure 5.—Continued

data for sound velocity included re-computation of depth from the measured acoustic pulse travel time using the vertical profile of sound velocity, rather than just the surface sound velocity, and re-mapping the placement of individual point measurements relative to the echosounder to compensate for refraction of the acoustic beams as they traveled through layers of water with different sound velocities. During data collection with the multibeam echosounder, sound velocity was also measured near the surface with the SVP 70. PDS was used to combine the time series of measurements of sound velocity at the surface with the average sound velocity profile over depth to form a time series of sound velocity profiles and apply corrections to the measured points. At many reservoirs, only one average sound velocity profile was needed if data were collected over a short period of time and the shape of the reservoir created a consistent profile of sound velocity. Multiple average sound velocity profiles were required when data were collected over a long period of time or when the reservoir contained areas of water largely physically disconnected from each other, for example by road causeways (for example, Croton Falls Reservoir) or by reservoir geometry (for example, Kensico Reservoir).

Depths measured by the MB2 were converted to elevations above NAVD 88 using the water surface elevation as a reference. A moving average of the time series of the water surface elevation at the pressure transducer (recorded at 15-minute intervals) was computed using a 1-hour-and-15-minute- (five-observation)-centered window to remove noise (for example, from waves near the pressure transducer) from the time series. Surveyed depths were then subtracted from the time series of the water surface elevation to compute bathymetric elevations.

Table 5. Summary of the velocity profiles groups used to measure bathymetry in New York City's East of Hudson reservoirs and controlled lakes, in Westchester and Putnam Counties, New York.

[Locations of reservoirs shown on figure 1. Survey data are available in Nystrom and others (2021)]

Sound velocity profile group	Date range	Area applied
	Amawalk Reservoir	
Amawalk_20180516_21	5/16/2016–5/21/2018	Whole reservoir
Amawalk_20191104_06	11/4/2019–11/6/2019	Whole reservoir
	Bog Brook Reservoir	
BogBrook_20171027	10/27/2017	Whole reservoir
BogBrook_20171031	10/31/2017	Whole reservoir
	Boyd Corners Reservoir	
Boyd_20170927_28	9/27/2017–9/28/2017	Whole reservoir
	Cross River Reservoir	
CrossRiver_20180619_21	6/19/2018–6/21/2018	Main basin
CrossRiver_20180625_27	6/25/2018–6/27/2018	Main basin
CrossRiver_EastCutoff_20191021	10/21/2019	East cutoff of main basin
	Croton Falls Reservoir	
CrotonFalls_WestBasin_20170829_30	8/29/2017–8/30/2017	West basin
CrotonFalls_EastBasin_20170831	8/31/2017	East basin
CrotonFalls_NorthBasin_20180514	5/14/2018	North basin
CrotonFalls_NorthBasinWestCutoff_20191023	10/23/2019	West cutoff of north basin
CrotonFalls_SouthCutoff_20191024	10/24/2019	South cutoff of west basin
	Diverting Reservoir	
Diverting_20170626_27	6/26/2017–6/27/2017	Main basin
Diverting_20170627_Inlet	6/27/2017	Inlet
	East Branch Reservoir	
EastBranch_20180523_25	5/23/2018–5/23/2018	Main basin
EastBranch_20180618	6/18/2018	Main basin
Eastbranch_NorthCutoff_20191023	10/23/2019	North cutoff of main basin
EastBranch_SouthCutoff_20191023	10/23/2019	South cutoff of main basin
	Lake Gilead	
Gilead_20170522_23	5/22/2017–5/23/2017	Whole lake
	Lake Gleneida	
Gleneida_20170524_25	5/24/2017–5/25/2017	Whole lake
	Kensico Reservoir	
Kensico_Delaware_20180627	6/27/2018	Delaware tunnel inflow
Kensico_MainBay_20180627_29	6/27/2018–6/29/2018	Main bay
Kensico_Ring_20180627_29	6/27/2018–6/29/2018	Ring around Great Island
Kensico_MainBay_20180717_20	7/17/2018–7/20/2018	Main bay
Kensico_Ring_20180718_19	7/18/2018–7/19/2018	Ring around Great Island
Kensico_DelawareOutlet_20180718_19	7/18/2018–7/19/2018	Delaware outlet channel
Kensico_Delaware_20180718_19	7/18/2018–7/19/2018	Delaware tunnel inflow
Kensico_NorthArm_20180720	7/20/2018	North arm
Kensico_Ring_20180726	7/26/2018	Ring around Great Island
Kensico_MainBay_20180726	7/26/2018	Main bay
Kensico_Middle_20180726	7/26/2018	Bay west of Cooney Hill

Table 5. Summary of the velocity profiles groups used to measure bathymetry in New York City's East of Hudson reservoirs and controlled lakes, in Westchester and Putnam Counties, New York.—Continued

[Locations of reservoirs shown on figure 1. Survey data are available in Nystrom and others (2021)]

Sound velocity profile group	Date range	Area applied
	Kensico Reservoir—Continued	
Kensico_MainBay_20180820_24	8/20/2018–8/24/2018	Main bay
Kensico_Rye_20180820_24	8/20/2018–8/24/2018	Rye Lake
Kensico_Middle_20180820_24	8/20/2018–8/24/2018	Bay west of Cooney Hill
Kensico_NorthArm_20180822_24	8/22/2018–8/24/2018	North arm
Kensico_Delaware _N_20180824	8/24/2018	Delaware outlet channel
Kensico_Delaware _Mid_20180824	8/24/2018	Delaware outlet channel
Kensico_Delaware _South_20180824	8/24/2018	Delaware outlet channel
Kensico_Ring_20180824	8/24/2018	Ring around Great Island
	Kirk Lake	
Kirk_20170622_23	6/22/2017–6/23/2017	Whole lake
	Middle Branch Reservoir	
MiddleBranch_20170728_0803	7/28/2017–8/3/2017	Whole reservoir
	Muscoot Reservoir	
Muscoot_20170605_09	6/5/2017–6/9/2017	Main basin
Muscoot_Bay_20170620_21	6/20/2017–6/21/2017	Bay
Muscoot_Narrow_20170620_21	6/20/2017–6/21/2017	Northern section of reservoir
Muscoot_Bay_20170620_21	6/20/2017–6/21/2017	Bay
Muscoot_20191107	11/7/2019	Main basin
	New Croton Reservoir	
NewCroton_20170628	6/28/2017	Whole reservoir
NewCroton_20170719_21	7/19/2017–7/21/2017	Whole reservoir
NewCroton_20170724_27	7/24/2017–7/27/2017	Whole reservoir
NewCroton_20171026	10/26/2017	Whole reservoir
	Titicus Reservoir	
Titicus_20171102_03	11/2/2017–11/3/2017	Whole reservoir
Titicus_20180515	5/15/2018	Whole reservoir
Titicus_20180522	5/22/2018	Whole reservoir
	West Branch Reservoir	
WestBranch_WestsBasin_20170918_25	9/18/2017–9/25/2017	West basin
WestBranch_EastBasin_20170925_26	9/25/2017–9/26/2017	East basin
WestBranch_WestBasin_20171025	10/25/2017	West basin
WestBranch_Cutoff_20191022	10/22/2019	East basin cutoff

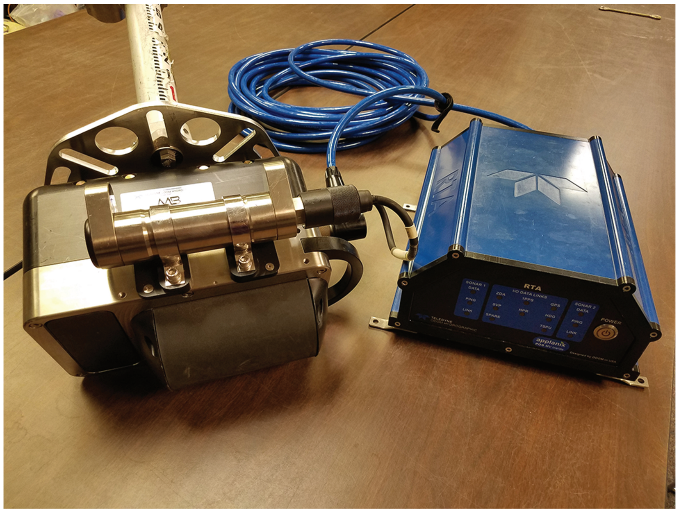

Figure 6. Photograph of a multibeam echosounder; photograph by Elizabeth Nystrom, U.S. Geological Survey.

The INS installed in the multibeam echosounder measures pitch, roll, heading, and heave to compute the correct location of the points measured by the MB2 in three-dimensional space. Review of recorded heave data during processing showed large variability (sometimes more than 3 ft) that did not reflect the observed vertical movement of the boat during data collection, which was minimal, leading to the removal of the heave correction from the data. Vertical position data collected with RTK GNSS with good satellite constellations were examined to verify that there was no observable vertical movement of the boat while underway due to the attitude of the boat (squat or planing). To calibrate the alignment of the pitch, roll, and heading sensors of the INS to the MB2, patch tests were performed during the surveys. A patch test consists of a series of movements recorded with a multibeam echosounder over a bathymetric surface: data are collected during two passes traveling in opposite directions over a flat surface to calibrate the roll correction, then two more passes traveling in opposite directions over a slope to calibrate the pitch correction, and two final passes traveling in the same direction along offset paths over a slope to calibrate the heading correction. There were 16 patch tests (table 6), and

Table 6. Multibeam echosounder patch test and calibration computation results for bathymetry measurements in New York City's East of Hudson reservoirs and controlled lakes, in Westchester and Putnam Counties, New York.

[Locations of reservoirs shown on figure 1. Survey data are available in Nystrom and others (2021). GNSS, global navigation satellite system; RTK, real-time kinematic corrections used; GPS, stand-alone GNSS or differential GNSS; —, not used]

Date	Reservoir	GNSS mode	Roll correction, degrees	Pitch correction, degrees,	Heading correction, degrees
Calibration group 1; May 2017 to July 2017					
6/27/2017	Diverting	RTK	−0.16	0.13	−3.07
6/29/2017	Muscoot	RTK	0.00	0.37	−2.59
6/22/2017	Kirk	GPS, some RTK	−0.22	0.05	−2.62
7/26/2017	New Croton	RTK, some GPS	−0.22	1.96	−3.13
Calibration group 2; August 2017 to May 2018					
8/30/2017	Croton Falls	RTK	0.01	0.24	−2.55
9/27/2017	Boyd Corners	GPS, some RTK	−0.21	0.30	—
5/16/2018	Amawalk	RTK	−0.21	0.60	−3.98
Calibration group 3; June 2018 to July 2018					
6/21/2018	Cross River	RTK	−0.17	0.23	0.34
7/18/2018	Kensico	RTK	−0.04	0.1	5.53
7/19/2018	Kensico	GPS	−0.07	0.33	6.19
7/19/2018	Kensico	RTK	−0.02	0.02	5.26
7/19/2018	Kensico	GPS	−0.07	0.26	5.84
7/19/2018	Kensico	RTK	−0.16	−0.58	5.57
7/20/2018	Kensico	RTK	−0.13	−0.75	6.50
Calibration group 4; August 2018					
8/23/2018	Kensico	RTK	0.00	0.77	5.55
Calibration group 5; November 2019					
11/5/2019	Amawalk	RTK	0.09	0.72	5.60

calibration values were calculated. The largest changes over time were to the calibrated heading corrections; some of these changes over time may have been due to small movements of the poles that the INS GNSS receivers were mounted on, resulting in changes to the GNSS receiver positions relative to the multibeam echosounder and INS. The patch test calibrations were then grouped into five date ranges, and average values of roll, pitch, and heading corrections were computed for each group.

The average group calibration values were applied to the MB2 data based on the date the MB2 data were collected. The results of the calibration fit were evaluated by examining the standard deviation of point values within grid cells; in some cases, the calibration results from an individual calibration were applied if the calibration results improved the alignment of the data points for the reservoir. In four of the reservoirs (table 7), a calibration value was hand-adjusted to better align data points based on overall improvement of the data for the reservoir; the multibeam echosounder data are most sensitive to adjustment of roll calibration, and this was usually the value that was adjusted. The final INS calibration values were used to process the multibeam echosounder data (table 7).

After correction for sound velocity, conversion to elevation, and calibration for heading, pitch, and roll, point data collected by the multibeam echosounder were edited to remove erroneous data and spikes. Point editing in PDS uses filters and manual editing. Filters use metadata about each return and the surrounding points and surface to identify spikes and points of poor quality, which are then reviewed and removed. Manual editing was largely used to remove points recorded above the reservoir bottom when the acoustic signal was reflected off aquatic plants.

The MB2 recorded more than 20 million swaths (each a single observation in time with up to 256 point observations) in the EOH reservoirs and controlled lakes (table 8), for a total of more than 5 billion points. About 28 percent of those points were rejected by filters and editing, including many in areas of dense aquatic plant growth, resulting in a total of almost 3.7 billion valid point observations after editing. A larger

Table 7. Final calibration values used to process multibeam echosounder data for bathymetry measurements in New York City's East of Hudson reservoirs and controlled lakes, in Westchester and Putnam Counties, New York.

[Locations of reservoirs shown on figure 1. Survey data are available in Nystrom and others (2021). avg, average group calibration; indiv, individual calibration; adj, calibration adjusted based on local reservoir data]

Reservoir	Date range	Roll correction, degrees	Pitch correction, degrees,	Heading correction, degrees	Notes
Amawalk Reservoir	May 2018	−0.14	0.38	−3.27	Group 2 avg
	November 2019	0.09	0.72	5.60	Group 5
Bog Brook Reservoir	October 2017	0.05	0.38	−3.27	Group 2 adj
Boyd Corners Reservoir	September 2017	−0.14	0.38	−3.27	Group 2 avg
Cross River Reservoir	June 2018	−0.17	0.23	0.34	Indiv
Croton Falls Reservoir	August 29 2017	0.03	0.32	−0.50	Indiv adj
	August 30, 2017; May 2018	0.01	0.24	−2.55	Indiv
Diverting Reservoir	June 2017	−0.16	0.13	−3.07	Indiv
East Branch Reservoir	May 2018	−0.14	0.38	−3.27	Group 2 avg
	June 2018	−0.09	−0.06	5.03	Group 3 avg
Lake Gilead	May 2017	−0.15	0.63	−2.85	Group 1 avg
Lake Gleneida	May 2017	−0.15	0.63	−2.85	Group 1 avg
Kensico Reservoir	June and July 2018	−0.09	−0.06	5.03	Group 3 avg
	August 2018	0.00	0.77	5.55	Indiv
Kirk Lake	June 2017	−0.22	0.05	−2.62	Indiv
Middle Branch Reservoir	July and August 2017	−0.15	0.63	−2.85	Group 1 avg
Muscoot Reservoir	June 2017	−0.15	0.63	−2.85	Group 1 avg
	November 2019	−0.15	0.72	5.60	Indiv adj
New Croton Reservoir	June and July 2017	−0.15	0.63	−2.85	Group 1 avg
	October 2017	−0.14	0.38	−3.27	Group 2 avg
Titicus Reservoir	November 2017; May 2018	0.05	0.38	−3.27	Group 2 adj
West Branch Reservoir	September and October 2017	−0.14	0.38	−3.27	Group 2 avg

Table 8. Multibeam echosounder swaths recorded and points used in bathymetric mapping for New York City's East of Hudson reservoirs and controlled lakes, in Westchester and Putnam Counties, New York.

[Locations of reservoirs shown on figure 1. Survey data are available in Nystrom and others (2021)]

Reservoir	Swaths recorded	Valid points after editing	Percent of possible points used
Amawalk Reservoir	1,241,742	212,039,627	67
Bog Brook Reservoir	500,215	109,839,383	86
Boyd Corners Reservoir	548,985	111,592,773	79
Cross River Reservoir	1,905,259	389,341,968	80
Croton Falls Reservoir	995,318	198,127,567	78
Diverting Reservoir	512,755	102,209,977	78
East Branch Reservoir	1,059,104	232,173,137	86
Lake Gilead	271,163	23,279,236	34
Lake Gleneida	463,824	44,934,534	38
Kensico Reservoir	3,189,588	634,632,623	78
Kirk Lake	876046	185,196,539	83
Middle Branch Reservoir	613,975	126,155,198	80
Muscoot Reservoir	2,472,702	388,065,707	61
New Croton Reservoir	2,345,130	400,057,133	67
Titicus Reservoir	1,102,892	167,477,387	59
West Branch Reservoir	1,914,853	367,962,147	75
Total	20,013,551	3,693,084,936	72

percentage of points than the average for all EOH reservoirs and controlled lakes were removed in some reservoirs mainly due to aquatic plant growth conditions (for example, in Lake Gilead, a substantial part of the lake was filled with weedy areas).

Acoustic Doppler Current Profiler

Additional bathymetric data were collected in October 2019 in small areas of Cross River, Croton Falls, East Branch, and West Branch Reservoirs (fig. 1) because they were inaccessible with the boat used for the multibeam echosounder surveys (which required a trailer); for the additional data collection, a Teledyne RD Instruments 1,200-kHz RioPro ADCP was used (Teledyne Marine, 2016). The ADCP was deployed in a small trimaran tethered to a small manned boat powered with an electric trolling motor (fig. 7) and deployed by hand. The additional data were reviewed using Teledyne

Figure 7. Photograph of bathymetry data collection with acoustic Doppler current profiler on October 23, 2019, at East Branch Reservoir in Putnam County, New York; photograph by Elizabeth Nystrom, U.S. Geological Survey.

RD Instruments WinRiver II version 2.18 (Teledyne Marine, 2020). The built-in self-tests that are included in WinRiver II were run daily before the start of data collection, and the water temperature measured by the ADCP was verified by an independent measurement using a thermistor.

Along with the ADCP depth data, position data were collected with a Hemisphere GNSS, Inc. V102 GNSS compass (Hemisphere GNSS, Inc., 2017) using differential GNSS. Position data were output from the V102 at 2 hertz (Hz) as NMEA 0183 $GPGGA strings (National Marine Electronics Association, 2002) and recorded as ASCII text files using WinRiver II. Surface sound velocity was calculated by WinRiver II for each ping by using the water temperature measured by the ADCP; sound velocity profiles were measured but varied by less than 0.5 percent from surface to bottom at all sites (fig. 5, profiles in pink [shallow profiles]). Consequently, sound velocity corrections over depth were not applied. The RioPro ADCP measured four individual acoustic beam depths for each ping, each similar to a single beam echosounder measurement; for mapping, an average of the four beam depth measurements was used because the areas measured were generally shallow and not steeply sloped. Depths measured by the ADCP were converted to elevations above NAVD 88 using the water surface elevation as a reference as with the multibeam echosounder data; however, for the ADCP measurements, constant values measured with static GNSS observations were used. After conversion to elevation, each transect was screened for spikes and measurement errors. More than 48,000 ADCP points were recorded and used in processing (table 9).

Table 9. Acoustic Doppler current profiler points used in bathymetric mapping for New York City's East of Hudson reservoirs and controlled lakes, in Westchester and Putnam Counties, New York.

[Locations of reservoirs shown on figure 1. Survey data are available in Nystrom and others (2021)]

Reservoir	Valid points after editing
Cross River Reservoir	10,414
Croton Falls Reservoir	17,979
East Branch Reservoir	10,184
West Branch Reservoir	10,035
Total	48,612

Figure 8. Photograph of a single-beam echosounder; photograph by Elizabeth Nystrom, U.S. Geological Survey.

Single-Beam Echosounder

Bathymetric data were collected with a single-beam echosounder at each reservoir for use as a quality-assurance check of the mapped multibeam echosounder data. The single-beam echosounder used for this study was a SyQwest Inc. Bathy-500MF (fig. 8) survey-grade echosounder with a resolution of 0.1 ft and a manufacturer-specified accuracy of 0.1 ft plus 0.1 percent of the depth (SyQwest, Inc., 2008). A 200-kHz narrow-beam transducer (3° at 3 decibels) was used; the minimum measurable depth with this configuration was approximately 3 ft. Position data were measured using the R8 GNSS receiver with VRS RTK corrections; the GNSS receiver was mounted directly above the single-beam transducer during data collection. Pitch and roll were not recorded or used in processing the single-beam echosounder data. Instead, the transducer was leveled on the boat using a bubble level attached to the transducer mount; errors in the alignment of the transducer or changes in the tilt of the boat while under way, therefore, can contribute to errors in measurement of depth with the single-beam echosounder (Nystrom and Collenburg, 2020).

Live echosounder readings and RTK GNSS positional data were integrated while in the field using HYPACK version 17.0.26.0 (HYPACK, 2021) hydrographic software, which used the NMEA 0183 $GPZDA string to temporally synchronize position and depth data with the GNSS data. Single-beam echosounder data were collected along predetermined transects oriented at a 45° angle to the main axis of the reservoir; the goal of the spacing of the transects was to record data along approximately 10 lines from edge to edge of the reservoir. The configuration of these quality assurance lines followed procedures similar to those used by Wilson and Richards (2006).

Single-beam echosounder data were processed using HYPACK version 19.0.11.0 (HYPACK, 2021); processing included correction for changes in sound velocity over depth, conversion from depth to elevation above NAVD 88 using the water surface elevation as a reference (same process as for the multibeam echosounder data), and manual editing to remove erroneous points or spikes. The averaged sound velocity profiles applicable to the date and location of the data collection were used to process the single-beam data. Depths measured by the single-beam echosounder were converted to elevations above NAVD 88 by using the same method as was used for the multibeam echosounder data, using the water surface elevation as a reference.

After conversion to elevation, each transect was screened for spikes and measurement errors. Spikes and errors can occur in the echo sounder data in the digitization process (the process by which the echosounder determines a digital depth value from the analog echo signal received by the transducer). For example, a strong return from objects in the water column (such as debris, fish, or vegetation) can be digitized as the measured depth, or the "second" acoustic return can be digitized instead of the "first." Errors can occur because in shallow water, sound can be reflected off the water surface as well as the reservoir bottom; the "second" return travels from the echosounder to the reservoir bottom, to the water surface, to the reservoir bottom, and back to the echosounder before being digitized; therefore, the recorded value is approximately twice as deep as the actual value. After processing the single-beam echosounder data, about 284,000 point observations remained (table 10).

Table 10. Single-beam echosounder points used in quality assurance of bathymetric mapping for New York City's East of Hudson reservoirs and controlled lakes, in Westchester and Putnam Counties, New York.

[Locations of reservoirs shown on figure 1. Survey data are available in Nystrom and others (2021)]

Reservoir	Valid points after editing
Amawalk Reservoir	15,271
Bog Brook Reservoir	18,711
Boyd Corners Reservoir	10,049
Cross River Reservoir	20336
Croton Falls Reservoir	27,847
Diverting Reservoir	8,845
East Branch Reservoir	20,142
Lake Gilead	5,945
Lake Gleneida	14,960
Kensico Reservoir	27,315
Kirk Lake	15,345
Middle Branch Reservoir	12,020
Muscoot Reservoir	16,808
New Croton Reservoir	18,568
Titicus Reservoir	17,669
West Branch Reservoir	33,916
Total	283,747

Bathymetric Map Creation

Complete coverage of the bathymetric surface with the multibeam echosounder was not possible, especially in shallow areas near shorelines where boat navigation was limited or in areas with excessive aquatic plants. Light detection and ranging (lidar) data (NYCDEP, 2009) were used to supplement the echosounder data along reservoir shorelines and islands and to allow interpolation of elevation in shallow areas near the edge of the reservoir. Lidar data were imported into ArcMap (Esri Inc., 2020) by extracting the ground returns from the point clouds in the LAS format file for an area around the reservoir bounded by the lidar contour line closest to 10 ft above the surveyed water surface elevation, with an additional surrounding buffer of 32.8 ft. Furthermore, all lidar data above the water surface elevation were included for islands within a given lake. The processed multibeam echosounder points were combined with ADCP data and the lidar data, and gaps were interpolated to create complete raster grid bathymetric surfaces. The raster grids were then used to create bathymetric contours and compute elevation-area-capacity tables and were compared with the quality assurance dataset. The raster grid bathymetric surfaces and contours were created in the Grid Model Editor of the PDS software (Teledyne PDS, 2019, §19.2).

A 3.28-ft cell-size raster grid was created for each data source (multibeam echosounder, ADCP, and lidar) using the mean elevation of the points within a given raster cell; these single-source grids were then combined into a single raster grid, with multibeam echosounder data taking precedence over other data sources, and ADCP data taking precedence over lidar data. Grid cells computed using multibeam echosounder data contained an average of about 92 individual measurements of depth. The number of multibeam echosounder measurements in a given area is dependent on the water depth, the ping rate and beam geometry of the echosounder, the speed of the boat, and the overlap of successive measurement passes. In general, the echosounder can make more measurements per unit time in shallow water and a single measurement swath of points covers a smaller distance than it would in deeper water, and the overall number of multibeam echosounder measurements per cell is largely dependent on average depth. Of the EOH reservoirs and controlled lakes, Kirk Lake (which was fairly shallow) had the highest average multibeam echosounder point measurement density per grid cell (about 410; table 11) and Lake Gilead (which was fairly deep) had the lowest (about 57). Grid cells computed using lidar or ADCP data typically had one to two observations per cell.

Table 11. Summary of multibeam measurements in grid cells for New York City's East of Hudson reservoirs and controlled lakes, in Westchester and Putnam Counties, New York.

[Grid cell are 3.28-foot cells in the mapped raster grid of the bathymetric surface. Locations of reservoirs shown on figure 1. Survey data are available in Nystrom and others (2021)]

Reservoir	Number of multibeam grid cells	Mean number of measurements in each cell	Median number of measurements in each cell
Amawalk Reservoir	2,106,722	100.6	61
Bog Brook Reservoir	1,460,609	75.2	42
Boyd Corners Reservoir	745,916	149.6	88
Cross River Reservoir	3,323,054	117.2	64
Croton Falls Reservoir	3,242,971	61.1	31
Diverting Reservoir	520,343	196.4	103
East Branch Reservoir	1,878,839	123.6	58
Lake Gilead	405,324	57.4	24
Lake Gleneida	647,544	69.4	37
Kensico Reservoir	8,293,885	76.5	36
Kirk Lake	451,895	409.8	232
Middle Branch Reservoir	1,442,637	87.4	54
Muscoot Reservoir	2,202,971	176.2	126
New Croton Reservoir	7,035,332	56.9	36
Titicus Reservoir	2,293,188	73.0	43
West Branch Reservoir	3,906,979	94.2	50

The grid cells that did not contain any echosounder or lidar data were interpolated in the PDS Grid Model Editor (Teledyne PDS, 2019, §19.2), first using the circular interpolation function with a small interpolation radius (6.5 to 16.5 ft), and then filling the remaining larger gaps using the triangular interpolation method. The circulation interpolation routine is typically used to fill small gaps in the data; it computes an inverse-distance-weighted mean of cells within the interpolation radius (Teledyne PDS, 2019). The triangular interpolation routine creates a triangulated irregular network (also known as a TIN) to fill larger gaps in the data. An iterative process was used, in which an interpolation was run and examined; estimated points were added as necessary to create a visually reasonable interpolation.

Areas along and near structures such as dams and spillways, around submerged islands, near shorelines, and with a high density of submerged vegetation, where echosounder data could not be collected, were areas that typically required the addition of estimated points. The shape of the shoreline strongly influenced where estimated points were required; for example, estimated points were used to prevent large flat areas from being created due to triangulation connection of lidar data on opposite sides of inlet channels or shallow bays (fig. 9). The initial elevation values for estimated points in these areas were based on a linear interpolation between multibeam echosounder data and lidar data; in some cases, estimated values were drawn in to approximate the placement of an elevation contour. Some of the largest interpolation areas that required the addition of estimated points were shallow areas with a large amount of submerged vegetation where echosounder data could not be collected, for example, the many shallow bays in Muscoot Reservoir. Echosounder data were collected as far into these shallow areas as possible to characterize the slope and shape of the reservoir bottom in those parts of the area and to determine the location and depth of any channels. Many of the largest shallow weedy areas were very flat, which informed the estimation of the unmeasurable areas. Additionally, aerial orthophotographs were

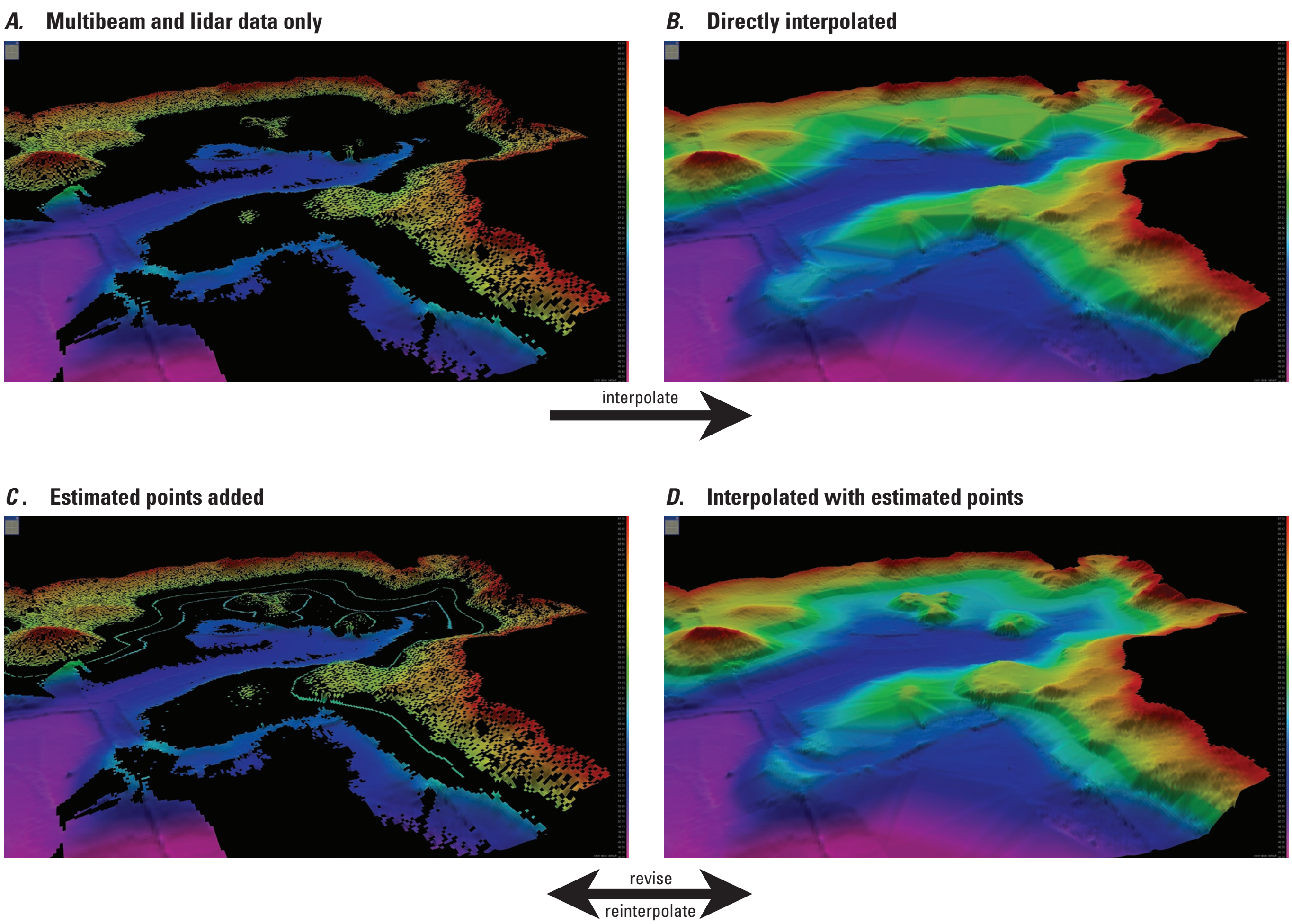

Figure 9. Maps showing example of interpolation between multibeam echosounder data and light detection and ranging (lidar) data with and without estimated points for bathymetry measurements in New York City's East of Hudson reservoirs and controlled lakes, in Westchester and Putnam Counties, New York. *A*, Multibeam and lidar data only; *B*, interpolated from multibeam and lidar data; *C*, estimated points added; and *D*, interpolated with estimated points added. Arrows indicate direction of processing step.

used to identify the shape of submerged features and inlets, the location of extremely shallow areas, and to estimate the maximum elevation of submerged islands relative to spillway elevations.

Two additional raster grids were created for each reservoir to describe the data contained in the elevation grid: one that contains information about the source of the data used in the final elevation grid, and one that contains the standard deviation of the point elevation values within each cell. The sizes and locations for the cells in these grids were created to match those of the elevation grids. The raster grid of source data type contains an enumerated value that specified if the elevation was determined with the multibeam echosounder, ADCP, or lidar data or if it contained an estimated or interpolated value. The standard deviation grid (Nystrom and others, 2021) contains the standard deviation of observed point elevations within a cell; if a cell contained fewer than two elevation observations (for example, estimated or interpolated cells), the standard deviation for that cell could not be computed and it was left empty.

About 84 percent of the total surface area of the EOH reservoirs and controlled lakes was measured using the multibeam echosounder (table 12) and lidar data filled about 2 percent of the mapped reservoirs, requiring estimated and interpolated data for about 14 percent of the mapped reservoirs. Lidar data and interpolated cells were used to fill in the mapped area above the water surface, which was included to allow computation of reservoir capacity for elevations above spillway elevation. Lake Gleneida and Kensico Reservoir had the highest percentages of area directly measured with the multibeam echosounder (93 and 92 percent, respectively). Muscoot Reservoir had the lowest percentage of area directly measured with the multibeam echosounder (64 percent) and the highest percentage of estimated and interpolated area (35 percent) because of the extent of large, extremely weedy, shallow areas in the reservoir. The largest percentages of area covered with lidar data were at Diverting, East Branch, and Bog Brook Reservoirs (10, 11, and 7 percent, respectively); the water level at these three reservoirs was fairly low when the lidar data were collected, so more of the area between the shoreline and the multibeam echosounder data contained useable lidar data.

Bathymetric contours were created at 2-ft intervals of depth and elevation above NAVD 88 from the 3.28-ft raster using the Grid Model Editor in PDS (Teledyne PDS, 2019, §19.2). A smoothing window of 4 (medium) was used, and contours less than 20 ft long (about the length of the border of two grid cells) were removed. In some steep areas (for example, close-to-vertical dam faces or intake structures), contours were hand edited after they were created to prevent contours from crossing; along vertical structures, many contours were essentially coincident. Elevation-area-capacity tables were calculated from mapped raster surfaces in a geographic information system (GIS) using the surface volume three-dimensional analyst tool in ArcMap (Esri Inc., 2020). Capacity data were tabulated at 0.01-ft intervals from about 1 ft above the lowest mapped elevation—the lowest computed elevation was chosen to result in a computed volume of about 0.01 million gallons—to 4 ft above the spillway elevation. Capacity tables were computed for water surface elevations above spillway elevations because the water surface elevation in the reservoirs is often slightly higher than the spillway elevation when the reservoir is full and spilling and for emergency preparedness in case of flooding.

Table 12. Summary of percent of area mapped, by data source, for bathymetry measurements in New York City's East of Hudson reservoirs and controlled lakes, in Westchester and Putnam, New York.

[Locations of reservoirs shown on figure 1. Survey data are available in Nystrom and others (2021). Percentages shown are percent of mapped reservoir area at full spillway elevation. lidar, light detection and ranging; —, not applicable; <, less than]

Reservoir	Multibeam echosounder	Acoustic Doppler current profiler	Lidar	Estimated and interpolated
Amawalk Reservoir	88	—	<1	12
Bog Brook Reservoir	90	—	7	3
Boyd Corners Reservoir	81	—	1	18
Cross River Reservoir	88	<1	<1	11
Croton Falls Reservoir	82	<1	5	12
Diverting Reservoir	85	—	11	5
East Branch Reservoir	80	<1	10	9
Lake Gilead	88	—	<1	11
Lake Gleneida	93	—	<1	7
Kensico Reservoir	92	—	1	8
Kirk Lake	88	—	<1	12
Middle Branch Reservoir	82	—	<1	17
Muscoot Reservoir	64	—	1	35
New Croton Reservoir	81	—	1	19
Titicus Reservoir	83	—	<1	17
West Branch Reservoir	90	<1	<1	10
Overall East of Hudson reservoirs and controlled lakes[1]	84	<1	2	14

[1]Totals may not equal 100 percent because of independent rounding.

Results of Bathymetric Surveys

The results of the bathymetric surveys (figs. 10 to 25, in back of report; table 13) show that depths at New York City's EOH reservoirs and controlled lakes range from about 25 ft (Kirk Lake) to about 162 ft (Kensico Reservoir). At full spillway elevation, the total capacity of the EOH reservoirs

Table 13. Summary of results of bathymetric surveys of New York City's East of Hudson reservoirs and controlled lakes, in Westchester and Putnam Counties, New York.

[Locations of reservoirs shown on figure 1. Expanded elevation-area-capacity table is available in Nystrom and others (2021). Values may not add to totals because of rounding. NAVD 88, North American Vertical Datum of 1988; —, not applicable]

Reservoir	Spillway elevation, in feet above NAVD 88	Maximum mapped depth, in feet	Total capacity at spillway elevation, in million gallons	Area at spillway elevation, in square miles	Area at spillway elevation, in acres
Amawalk Reservoir	398.32	74.37	6,731	0.9085	581.4
Bog Brook Reservoir	415.54	65.17	4,473	0.6284	402.2
Boyd Corners Reservoir	579.29	44.24	1,700	0.3469	222
Cross River Reservoir	328.23	114.17	10,350	1.431	915.6
Croton Falls Reservoir	307.83	108.36	13,950	1.693	1,084
Diverting Reservoir	308.11	35.58	814.3	0.2358	150.9
East Branch Reservoir	415.54	65.16	5,123	0.9024	577.5
Lake Gilead	492.60	113.74	1,859	0.1754	112.3
Lake Gleneida	501.00	100.57	2,709	0.268	171.5
Kensico Reservoir	355.98	161.67	41,200	3.466	2,218
Kirk Lake	585.63	25.59	574.0	0.2051	131.3
Middle Branch Reservoir	368.70	57.61	3,862	0.6585	421.4
Muscoot Reservoir	198.02	34.63	3,573	1.248	798.7
New Croton Reservoir	194.25	147.01	28,950	3.282	2,100
Titicus Reservoir	323.23	85.95	7,067	1.046	669.3
West Branch Reservoir	501.92	52.49	9,987	1.686	1,079
Total	—	—	142,920	18.181	11,635

and controlled lakes is about 142.9 billion gallons, with a total surface area of more than 11,600 acres (tables 13 and 14). The useable capacity of each reservoir (the volume above the minimum operating level for drinking water supply) was not computed but is less than the total capacity of the reservoir. GIS files of the bathymetry data, including the mapped bathymetric surfaces, contours, and quality assurance points, full capacity tables at 0.01-ft increments of elevation, and associated metadata are available in Nystrom and others (2021).

Accuracy Assessment

The accuracy of the mapped bathymetric data was evaluated using quality assurance datasets collected with a single-beam echosounder, as described in the "Quality Assurance Dataset: Single-beam Echosounder" section of this report, similar to methods described by Wilson and Richards (2006). About 284,000 quality assurance point observations were spatially joined with the mapped raster surfaces in a GIS, the measured elevations were compared (figs. 10*D* and *E* to 25*D* and *E*, in back of report), descriptive statistics were calculated. Two additional datasets were used for quality assurance of the bathymetric data in a part of the mapped area: a series of GNSS survey points recorded in Boyd Corners Reservoir and lidar data points along the shorelines of Bog Brook and East Branch Reservoirs. Both additional quality assurance datasets were recorded during periods of unusually low water levels. These two additional datasets allowed a quality assurance assessment with data sources that were more independent than the single-beam echosounder dataset because they did not require two of the processing steps used for the mapping data: the use of corrections for sound velocity over depth and the use of the water surface elevation as a reference to NAVD 88. In addition, the lidar dataset allowed a quality assurance assessment of the ADCP and single-beam echosounder datasets.

The National Standard for Spatial Data Accuracy (Federal Geographic Data Committee, 1998) defines a standard for assessing map accuracy based on the root mean square error (RMSE) of the data. Assuming the errors are normally distributed, the vertical accuracy of the map product can be calculated at the 95-percent accuracy level as 1.96 times the RMSE. Because it is not possible to separate the effects of many different factors on each measured point in the dataset, this accuracy assessment includes the cumulative effects of many potential sources of errors or inaccuracies in the multibeam and reference quality assurance datasets; these can include inaccuracies in the measurements of depth, position, attitude of the boat (pitch, roll, heading, and heave), sound velocity, time synchronization errors, and other sources of measurement error.

Table 14. Reservoir area and capacity at specified elevations for New York City's East of Hudson reservoirs and controlled lakes, in Westchester and Putnam Counties, New York.

[Locations of reservoirs shown on figure 1. Expanded elevation-area-capacity for the reservoirs and controlled lakes are available in Nystrom and others (2021). NAVD 88, North American Vertical Datum of 1988]

Elevation, in feet above NAVD 88	Depth below spillway, in feet	Capacity, in million gallons	Area, in square miles	Area, in acres
Amawalk Reservoir				
402.32	−4	7,509	0.9536	610.3
398.32	0	6,731	0.9085	581.4
388.32	10	4,968	0.7719	494
378.32	20	3,509	0.6359	407
368.32	30	2,329	0.4915	314.6
358.32	40	1,419	0.3919	250.8
348.32	50	689.9	0.3027	193.8
338.32	60	183.3	0.173	110.7
328.32	70	0.3604	0.002664	1.705
Bog Brook Reservoir				
419.54	−4	5,004	0.6471	414.2
415.54	0	4,473	0.6284	402.2
405.54	10	3,230	0.5638	360.8
395.54	20	2,126	0.4945	316.5
385.54	30	1,168	0.4215	269.8
375.54	40	392.9	0.3075	196.8
365.54	50	66.06	0.0358	22.91
355.54	60	10.17	0.01931	12.36
Boyd Corners				
583.29	−4	2,003	0.3758	240.5
579.29	0	1,700	0.3469	222
569.29	10	1,045	0.281	179.8
559.29	20	529.3	0.2087	133.5
549.29	30	170.5	0.1346	86.14
539.29	40	6.826	0.02792	17.87
Cross River Reservoir				
332.23	−4	11,580	1.508	965.1
328.23	0	10,350	1.431	915.6
318.23	10	7,553	1.238	792.4
308.23	20	5,212	1.012	647.4
298.23	30	3,327	0.7829	501
288.23	40	1,934	0.5581	357.2
278.23	50	1,040	0.3064	196.1
268.23	60	602.2	0.134	85.77
258.23	70	384.1	0.08973	57.43
248.23	80	217.1	0.07027	44.97

Table 14. Reservoir area and capacity at specified elevations for New York City's East of Hudson reservoirs and controlled lakes, in Westchester and Putnam Counties, New York.—Continued

[Locations of reservoirs shown on figure 1. Expanded elevation-area-capacity for the reservoirs and controlled lakes are available in Nystrom and others (2021). NAVD 88, North American Vertical Datum of 1988]

Elevation, in feet above NAVD 88	Depth below spillway, in feet	Capacity, in million gallons	Area, in square miles	Area, in acres
Cross River Reservoir—Continued				
238.23	90	95.08	0.04613	29.52
228.23	100	21.94	0.02402	15.37
218.23	110	0.6483	0.001887	1.208
Croton Falls Reservoir				
311.83	−4	15,400	1.778	1,138
307.83	0	13,950	1.693	1,084
297.83	10	10,690	1.44	921.6
287.83	20	7,973	1.151	736.7
277.83	30	5,883	0.8728	558.6
267.83	40	4,240	0.7052	451.3
257.83	50	2,906	0.5748	367.9
247.83	60	1,827	0.4698	300.7
237.83	70	959	0.3534	226.1
227.83	80	361.3	0.2219	142
217.83	90	49.7	0.07916	50.66
207.83	100	0.3922	0.000972	0.6219
Diverting Reservoir				
312.11	−4	1,019	0.258	165.1
308.11	0	814.3	0.2358	150.9
298.11	10	392	0.1679	107.5
288.11	20	113.8	0.09867	63.15
278.11	30	2.518	0.01056	6.759
East Branch Reservoir				
419.54	−4	6,005	1.26	806.2
415.54	0	5,123	0.9024	577.5
405.54	10	3,459	0.7142	457.1
395.54	20	2,172	0.4976	318.5
385.54	30	1,263	0.3774	241.5
375.54	40	602	0.255	163.2
365.54	50	188.6	0.1506	96.39
355.54	60	6.562	0.022	14.08
Lake Gilead				
496.6	−4	2,013	0.1932	123.7
492.6	0	1,859	0.1754	112.3
482.6	10	1,513	0.1555	99.51
472.6	20	1,213	0.1355	86.73

Table 14. Reservoir area and capacity at specified elevations for New York City's East of Hudson reservoirs and controlled lakes, in Westchester and Putnam Counties, New York.—Continued

[Locations of reservoirs shown on figure 1. Expanded elevation-area-capacity for the reservoirs and controlled lakes are available in Nystrom and others (2021). NAVD 88, North American Vertical Datum of 1988]

Elevation, in feet above NAVD 88	Depth below spillway, in feet	Capacity, in million gallons	Area, in square miles	Area, in acres
Lake Gilead—Continued				
462.6	30	948.8	0.1137	72.78
452.6	40	730.5	0.09681	61.96
442.6	50	542	0.08463	54.17
432.6	60	377.8	0.07238	46.32
422.6	70	240.9	0.05863	37.52
412.6	80	134.3	0.0435	27.84
402.6	90	59.33	0.02915	18.66
392.6	100	12.92	0.0132	8.448
382.6	110	0.612	0.001606	1.028
Lake Gleneida				
505	−4	2,938	0.2787	178.4
501	0	2,709	0.268	171.5
491	10	2,176	0.2414	154.5
481	20	1,703	0.2164	138.5
471	30	1,275	0.1946	124.6
461	40	898.6	0.1625	104
451	50	594.4	0.1326	84.85
441	60	342.2	0.1082	69.27
431	70	160.6	0.0634	40.58
421	80	60.17	0.03441	22.02
411	90	13.68	0.01195	7.648
401	100	0.02733	0.000588	0.3764
Kensico Reservoir				
359.98	−4	44,160	3.636	2,327
355.98	0	41,200	3.466	2,218
345.98	10	34,330	3.109	1,989
335.98	20	28,260	2.707	1,733
325.98	30	23,070	2.288	1,465
315.98	40	18,600	2.004	1,283
305.98	50	14,730	1.715	1,098
295.98	60	11,410	1.47	940.9
285.98	70	8,663	1.142	730.6
275.98	80	6,554	0.9366	599.4
265.98	90	4,727	0.8041	514.7
255.98	100	3,175	0.6841	437.8
245.98	110	1,915	0.4857	310.8

Table 14. Reservoir area and capacity at specified elevations for New York City's East of Hudson reservoirs and controlled lakes, in Westchester and Putnam Counties, New York.—Continued

[Locations of reservoirs shown on figure 1. Expanded elevation-area-capacity for the reservoirs and controlled lakes are available in Nystrom and others (2021). NAVD 88, North American Vertical Datum of 1988]

Elevation, in feet above NAVD 88	Depth below spillway, in feet	Capacity, in million gallons	Area, in square miles	Area, in acres
Kensico Reservoir—Continued				
235.98	120	1,115	0.3169	202.8
225.98	130	550.4	0.2214	141.7
215.98	140	179	0.1316	84.25
205.98	150	17.08	0.03009	19.26
195.98	160	0.01211	0.00015	0.096
Kirk Lake				
589.63	−4	817.4	0.3654	233.9
585.63	0	574	0.2051	131.3
575.63	10	228.6	0.1324	84.74
565.63	20	16.88	0.04861	31.11
Middle Branch Reservoir				
372.7	−4	4,428	0.6958	445.3
368.7	0	3,862	0.6585	421.4
358.7	10	2,589	0.5599	358.3
348.7	20	1,530	0.4578	293
338.7	30	688.4	0.3387	216.7
328.7	40	146.2	0.1678	107.4
318.7	50	1.215	0.002277	1.457
Muscoot Reservoir				
202.02	−4	4,722	1.487	951.6
198.02	0	3,573	1.248	798.7
188.02	10	1,496	0.7984	511
178.02	20	267.6	0.3294	210.8
168.02	30	5.821	0.02121	13.58
New Croton Reservoir				
198.25	−4	31,770	3.466	2,218
194.25	0	28,950	3.282	2,100
184.25	10	22,560	2.851	1,825
174.25	20	17,090	2.384	1,526
164.25	30	12,600	1.884	1,206
154.25	40	9,367	1.244	796.2
144.25	50	7,120	0.9481	606.8
134.25	60	5,354	0.7669	490.8
124.25	70	3,902	0.6282	402.1
114.25	80	2,739	0.4934	315.7
104.25	90	1,813	0.3865	247.4

Table 14. Reservoir area and capacity at specified elevations for New York City's East of Hudson reservoirs and controlled lakes, in Westchester and Putnam Counties, New York.—Continued

[Locations of reservoirs shown on figure 1. Expanded elevation-area-capacity for the reservoirs and controlled lakes are available in Nystrom and others (2021). NAVD 88, North American Vertical Datum of 1988]

Elevation, in feet above NAVD 88	Depth below spillway, in feet	Capacity, in million gallons	Area, in square miles	Area, in acres
New Croton Reservoir—Continued				
94.25	100	1,105	0.3	192
84.25	110	555.5	0.2218	142
74.25	120	202.3	0.1059	67.75
64.25	130	63	0.03995	25.57
54.25	140	8.155	0.01391	8.9
Titicus Reservoir				
327.23	−4	7,970	1.116	714
323.23	0	7,067	1.046	669.3
313.23	10	5,055	0.876	560.6
303.23	20	3,409	0.7002	448.1
293.23	30	2,122	0.5371	343.7
283.23	40	1,186	0.3664	234.5
273.23	50	549.6	0.2357	150.8
263.23	60	191.4	0.1216	77.85
253.23	70	26.15	0.03079	19.71
243.23	80	1.145	0.002669	1.708
West Branch Reservoir				
505.92	−4	11,430	1.765	1,129
501.92	0	9,987	1.686	1,079
491.92	10	6,659	1.503	961.7
481.92	20	3,762	1.262	807.9
471.92	30	1,534	0.7894	505.2
461.92	40	334.8	0.3785	242.3
451.92	50	0.4866	0.003615	2.314

Single-Beam Echosounder Dataset

Elevation measurement errors were calculated by subtracting the mapped raster surface elevation from the measured single-beam echosounder point elevation whenever a single-beam echosounder point fell within a mapped 3.28-ft grid cell; descriptive statistics were then calculated for each reservoir (tables 15 and 16). The mean error for all mapped quality assurance points in the EOH reservoirs and controlled lakes was 0.35 ft and ranged from 0.12 ft at Middle Branch and Muscoot Reservoirs to 0.63 ft at Kensico Reservoir. The 95-percent accuracy (computed from the RMSE of the errors) for all mapped single-beam echosounder quality assurance points in the EOH reservoirs and controlled lakes was 1.68 ft and ranged from 0.58 ft at Bog Brook Reservoir to 2.92 ft at New Croton Reservoir. The elevations measured with the single-beam echosounder averaged slightly above (shallower than) the elevation measured with the multibeam echosounder (positive errors; figs. 10*D* to 25*D*, in back of report). Sloped areas of a reservoir bottom can cause a shallow bias in single-beam echosounder measurements compared with multibeam echosounder measurements because of the acoustic beam width and the typical incidence angle of the acoustic beams; this effect is illustrated in Nystrom and Collenburg (2020).

The quality assurance points were categorized by the grid cell data source, and accuracy statistics were recomputed by category. The 95-percent accuracy of the areas measured with the multibeam echosounder was 1.67 ft (table 15); the accuracy in the areas where the data were interpolated was 2.74 ft, and the accuracy in the areas where the data were derived from lidar was 0.56 ft. The accuracy statistics were also categorized by the slope of the mapped surface (table 16); in very flat areas (slope less than 1°), the overall 95-percent accuracy was 0.55 ft compared with 6.63 ft in areas with slopes of 30° to 40°. In addition, the steeper the slope of the mapped surface, the larger the mean error, with the single-beam echosounder quality assurance points plotting shallower on average (table 16, positive mean errors). Mapping in steep areas may easily result in large errors because even small errors in time synchronization or measurement of boat position and attitude or in the position of the measured point within the mapped cell can result in large errors in measured depth. In addition, the single-beam echosounder has a wider acoustic beam than the multibeam echosounder, and the geometry of the beams and how they are reflected from the reservoir bottom can cause the single-beam echosounder to measure a shallower depth than the multibeam echosounder (Nystrom and Collenburg, 2020).

Because the capacity, or volume, of a reservoir represents a spatial average of the depth measurements, the accuracy of the computed capacity can be assessed by calculating confidence intervals around the mean error of the quality assurance points compared to the grids. This accuracy assessment of the capacity is calculated using the sample mean error and variance, as adapted from Helsel and others (2020) and as shown in Nystrom (2018). For the EOH reservoirs and controlled lakes, the confidence interval of the computed capacity at spillway elevation at 95-percent accuracy level was ±1.6 percent or less (table 17).

Table 15. Accuracy assessment of elevations of single-beam echosounder quality assurance points compared with mapped raster surfaces for bathymetric surveys of New York City's East of Hudson reservoirs and controlled lakes, in Westchester and Putnam Counties, New York.

[Locations of reservoirs shown on figure 1. Survey data are available in Nystrom and others (2021). $RMSE_z$, vertical root mean square error; $accuracy_z$, National Standard for Spatial Data Accuracy fundamental vertical accuracy calculated at the 95-percent confidence level; lidar, light detection and ranging]

Grid cell data source	Number of points	Mean error, in feet	Median error, in feet	$RMSE_z$, in feet	$Accuracy_z$, in feet
		Amawalk Reservoir			
Overall	15,271	0.45	0.36	1.02	2.00
Multibeam echosounder	15,133	0.45	0.36	1.01	1.98
Interpolated	138	0.47	0.17	1.71	3.35
		Bog Brook Reservoir			
Overall	18,711	0.15	0.12	0.30	0.58
Multibeam echosounder	18,324	0.15	0.12	0.30	0.58
Lidar	288	−0.06	−0.08	0.25	0.49
Interpolated	99	0.00	−0.06	0.46	0.90
		Boyd Corners Reservoir			
Overall	10,049	0.25	0.22	0.38	0.74
Multibeam echosounder	9,972	0.25	0.21	0.38	0.74
Interpolated	77	0.41	0.49	0.55	1.07
		Cross River Reservoir			
Overall	20,336	0.24	0.14	0.56	1.11
Multibeam echosounder	20,261	0.24	0.14	0.56	1.11
Interpolated	75	0.24	0.23	0.71	1.40
		Croton Falls Reservoir			
Overall	27,847	0.53	0.22	1.25	2.44
Multibeam echosounder	27,539	0.53	0.22	1.25	2.44
Lidar	127	−0.02	−0.07	0.22	0.43
Interpolated	181	0.78	0.17	1.72	3.37
		Diverting Reservoir			
Overall	8,845	0.18	0.17	0.47	0.93
Multibeam echosounder	8,589	0.19	0.17	0.47	0.92
Lidar	195	−0.10	−0.06	0.37	0.72
Int	61	0.58	0.57	1.05	2.06
		East Branch Reservoir			
Overall	20,142	0.37	0.23	0.69	1.36
Multibeam echosounder	20,104	0.37	0.23	0.69	1.36
Interpolated	38	0.94	0.79	1.30	2.54
		Lake Gilead			
Overall	5,945	0.32	0.24	1.23	2.41
Multibeam echosounder	5,823	0.32	0.24	1.23	2.41
Interpolated	122	0.03	0.11	1.22	2.39
		Lake Gleneida			
Overall	14,960	0.51	0.42	0.74	1.45
Multibeam echosounder	14,900	0.51	0.42	0.72	1.41
Interpolated	60	2.12	1.44	3.03	5.94

Table 15. Accuracy assessment of elevations of single-beam echosounder quality assurance points compared with mapped raster surfaces for bathymetric surveys of New York City's East of Hudson reservoirs and controlled lakes, in Westchester and Putnam Counties, New York.—Continued

[Locations of reservoirs shown on figure 1. Survey data are available in Nystrom and others (2021). $RMSE_z$, vertical root mean square error; $accuracy_z$, National Standard for Spatial Data Accuracy fundamental vertical accuracy calculated at the 95-percent confidence level; lidar, light detection and ranging]

Grid cell data source	Number of points	Mean error, in feet	Median error, in feet	$RMSE_z$, in feet	$Accuracy_z$, in feet
Kensico Reservoir					
Overall	27,315	0.63	0.37	1.20	2.35
Multibeam echosounder	27,213	0.63	0.37	1.19	2.34
Interpolated	102	0.78	0.24	1.82	3.56
Kirk Lake					
Overall	15,345	0.17	0.11	0.43	0.84
Multibeam echosounder	15,227	0.16	0.11	0.42	0.83
Interpolated	118	0.62	0.56	0.95	1.86
Middle Branch Reservoir					
Overall	12,020	0.12	0.11	0.34	0.67
Multibeam echosounder	11,977	0.12	0.11	0.34	0.66
Interpolated	43	0.42	0.15	0.92	1.80
Muscoot Reservoir					
Overall	16,808	0.12	0.14	0.35	0.68
Multibeam echosounder	16,667	0.12	0.14	0.34	0.67
Interpolated	141	0.32	0.24	0.81	1.58
New Croton Reservoir					
Overall	18,568	0.46	0.15	1.49	2.92
Multibeam echosounder	18,446	0.46	0.15	1.48	2.91
Interpolated	122	0.94	0.50	2.23	4.37
Titicus Reservoir					
Overall	17,669	0.52	0.37	0.95	1.86
Multibeam echosounder	17,563	0.52	0.37	0.95	1.86
Interpolated	106	0.61	0.59	1.18	2.30
West Branch Reservoir					
Overall	33,916	0.25	0.22	0.47	0.92
Multibeam echosounder	33,717	0.25	0.22	0.47	0.92
Interpolated	199	0.30	0.20	0.64	1.25
All East of Hudson reservoirs and controlled lakes					
Overall	283,747	0.35	0.21	0.86	1.68
Multibeam echosounder	281,455	0.35	0.21	0.85	1.67
Lidar	610	−0.06	−0.07	0.29	0.56
Interpolated	1,682	0.54	0.30	1.40	2.74

Table 16. Accuracy assessment of elevations of single-beam echosounder quality assurance points compared with mapped raster surfaces, categorized by slope, for bathymetric surveys of New York City's East of Hudson reservoirs and controlled lakes, in Westchester and Putnam Counties, New York.

[Locations of reservoirs shown on figure 1. Survey data are available in Nystrom and others (2021). $RMSE_z$, vertical root mean square error; $accuracy_z$, National Standard for Spatial Data Accuracy fundamental vertical accuracy calculated at the 95-percent confidence level]

Slope, in degrees	Number of points	Mean error, in feet	Median error, in feet	$RMSE_z$, in feet	$Accuracy_z$, in feet
0 to 1	85,401	0.17	0.15	0.28	0.55
>1 to 10	154,846	0.28	0.21	0.59	1.16
>10 to 20	32,724	0.73	0.49	1.41	2.77
>20 to 30	8,412	1.58	1.22	2.51	4.92
>30 to 40	2,254	2.39	1.97	3.38	6.63
>40 to 50	94	2.63	2.74	4.17	8.18
>50 to 60	15	5.53	3.9	7.85	15.39

Table 17. Accuracy assessment of computed capacity at spillway elevation for bathymetric surveys of New York City's East of Hudson reservoirs and controlled lakes, in Westchester and Putnam Counties, New York.

[Locations of reservoirs shown on figure 1. Survey data are available in Nystrom and others (2021). Mean error and variance computed by comparing single beam echosounder point elevations to mapped raster surfaces. Confidence intervals calculated at 95-percent level]

Reservoir	Mean error, in feet	Variance, in $feet^2$	Confidence interval of mean elevation, in feet	Confidence interval of capacity at spillway elevation, in millions of gallons	Confidence interval of capacity at spillway elevation, in percent
Amawalk Reservoir	0.45	0.84	±0.46	±87.7	±1.3
Bog Brook Reservoir	0.15	0.07	±0.15	±19.9	±0.4
Boyd Corners Reservoir	0.25	0.08	±0.26	±18.7	±1.1
Cross River Reservoir	0.24	0.26	±0.25	±74.3	±0.7
Croton Falls Reservoir	0.53	1.28	±0.54	±190.4	±1.4
Diverting Reservoir	0.18	0.19	±0.19	±9.5	±1.2
East Branch Reservoir	0.37	0.35	±0.38	±70.9	±1.4
Lake Gilead	0.32	1.41	±0.35	±12.7	±0.7
Lake Gleneida	0.51	0.29	±0.52	±29.2	±1.1
Kensico Reservoir	0.63	1.04	±0.64	±463.8	±1.1
Kirk Lake	0.17	0.16	±0.17	±7.5	±1.3
Middle Branch Reservoir	0.12	0.10	±0.12	±16.9	±0.4
Muscoot Reservoir	0.12	0.11	±0.13	±33.1	±0.9
New Croton Reservoir	0.46	2.01	±0.48	±328.9	±1.1
Titicus Reservoir	0.52	0.63	±0.53	±116.2	±1.6
West Branch Reservoir	0.25	0.16	±0.26	±90.1	±0.9

GNSS and Lidar Datasets

A set of GNSS survey points was recorded by the NYCDEP at Boyd Corners Reservoir during a period of low water levels in 2020. GNSS points were collected using NYSNet VRS RTK corrections on the reservoir bottom as much as 35 ft below the spillway elevation; 185 points were recorded that overlapped with the bathymetric surface mapped for this study, including 139 points that overlapped with the multibeam data (table 18). The mean error of the GNSS points compared with the mean error in areas measured with the multibeam echosounder was −0.02 ft, and the 95 percent accuracy was 0.86 ft.

The lidar data used in this study (NYCDEP, 2009) were collected during a period of low water levels (about 30 ft below the spillway elevation) at Bog Brook and East Branch Reservoirs. Although this overlap of lidar data and the surveyed areas was limited to a shallow portion of these two reservoirs, and therefore does not represent the full range of survey conditions in the EOH reservoirs and controlled lakes, it allowed for a quality assurance assessment of the single-beam echosounder data and the ADCP data. Individual lidar data points from the LAS files were spatially joined to mapped raster surfaces and to single-beam echosounder points within a 1-ft radius of a lidar data point. Because individual lidar data points were used, the user should be aware that some variability is inherent in these single point measurements; the metadata for the lidar dataset specifies that the RMSE of the lidar points compared with ground control checkpoints was less than 0.61 ft (NYCDEP, 2009).

The 95 percent accuracy computed by comparing the elevations of the lidar data points with those in the grid cells mapped with the multibeam echosounder was similar to that computed using the single-beam echosounder points (table 19). The mean error of the lidar data points compared with the ADCP data at East Branch Reservoir was −0.24 ft, and the 95 percent accuracy was 0.78 ft. The mean error of the lidar data points compared with those from the single-beam echosounder was very close to 0, and the computed 95 percent accuracy was about 1 ft, similar to that calculated for the multibeam echosounder data. As was observed in the comparison of single-beam echosounder data and multibeam echosounder data (table 20), the 95-percent accuracy of the lidar data points compared with those from the single-beam echosounder was better in flat areas than in steep areas: for example, accuracy of 0.47 ft in areas with slope less than 1° compared with 3.93 ft in areas with slope of 30° to 40°. Additionally, the steeper the slope of the mapped surface, the larger the mean error, with the single-beam echosounder points, especially, plotting on average shallower than the lidar data points in steeper areas (table 20, negative mean errors).

Table 18. Accuracy assessment of elevations of GNSS points compared with mapped raster surfaces for Boyd Corners Reservoir.

[Locations of reservoirs shown on figure 1. Survey data are available in Nystrom and others (2021). Each GNSS point was compared to the corresponding elevation of mapped raster; $RMSE_z$, vertical root mean square error; $accuracy_z$, National Standard for Spatial Data Accuracy fundamental vertical accuracy calculated at the 95-percent confidence level; lidar, light detection and ranging]

Grid cell data source	Number of points	Mean error, in feet	Median error, in feet	$RMSE_z$, in feet	$Accuracy_z$, in feet
Overall	185	−0.21	−0.02	0.88	1.72
Multibeam echosounder	139	−0.02	0.02	0.44	0.86
Lidar	2	−0.76	−0.76	0.78	1.52
Interpolated	44	−0.78	−0.87	1.62	3.17

Table 19. Accuracy assessment of elevations of lidar points compared with mapped raster surfaces and single-beam echosounder points at Bog Brook and East Branch Reservoirs in Putnam County, New York.

[Locations of reservoirs shown on figure 1. Survey data are available in Nystrom and others (2021). $RMSE_z$, vertical root mean square error; $accuracy_z$, National Standard for Spatial Data Accuracy fundamental vertical accuracy calculated at the 95-percent confidence level; ADCP, acoustic Doppler current profiler]

Data source	Number of points	Mean error, in feet	Median error, in feet	$RMSE_z$, in feet	$Accuracy_z$, in feet
Bog Brook Reservoir					
Multibeam echosounder grid cell	574,677	0.26	0.27	0.4	0.78
Interpolated grid cell	8,229	0.07	0.06	0.38	0.74
Single-beam echosounder points	2,103	−0.02	0.06	0.49	0.96
East Branch Reservoir					
Multibeam echosounder grid cell	1,297,421	0.33	0.35	0.5	0.98
ADCP grid cell	3,947	−0.24	−0.27	0.4	0.78
Interpolated grid cell	69,090	−0.32	−0.31	0.56	1.09
Single-beam echosounder points	3,533	0.02	0.08	0.57	1.11

Table 20. Accuracy assessment of elevations of lidar points compared with mapped multibeam raster cells and single-beam echosounder points, categorized by slope, at Bog Brook and East Branch Reservoirs in Putnam County, New York.

[Locations of reservoirs shown on figure 1. Survey data are available in Nystrom and others (2021). $RMSE_z$, vertical root mean square error; $accuracy_z$, National Standard for Spatial Data Accuracy fundamental vertical accuracy calculated at the 95-percent confidence level; >, greater than]

Slope, in degrees	Number of points	Mean error, in feet	Median error, in feet	$RMSE_z$, in feet	$Accuracy_z$, in feet
Multibeam echosounder grid cells					
0 to 1	56,823	0.21	0.22	0.37	0.73
>1 to 10	1,288,376	0.32	0.33	0.42	0.83
>10 to 20	452,867	0.33	0.34	0.51	1
>20 to 30	62,505	0.16	0.2	0.78	1.53
>30 to 40	9,733	0.11	0.17	1.13	2.22
>40 to 50	1,367	−0.08	0.04	1.48	2.91
>50 to 60	338	−0.5	−0.41	2.3	4.5
Single-beam echosounder points					
0 to 1	246	0.04	0.05	0.24	0.47
>1 to 10	3,250	0.1	0.11	0.37	0.72
>10 to 20	1,793	−0.03	−0.01	0.63	1.23
>20 to 30	316	−0.54	−0.6	1.07	2.09
>30 to 40	31	−1.59	−1.9	2	3.93

Summary

New York City's 16 East of Hudson reservoirs and controlled lakes were surveyed by the U.S. Geological Survey, in cooperation with the New York City Department of Environmental Conservation from May 2017 to November 2019 using a multibeam echosounder from a moving boat. Multibeam data were supplemented with acoustic Doppler current profiler data in some areas without boat ramps and with light detection and ranging (lidar) data above the water surface elevation. Quality-assurance datasets included single-beam echosounder data, global navigation satellite system (GNSS) point data, and lidar point data.

A Teledyne Odom MB2 multibeam echosounder with an integrated inertial navigation system using real-time sound velocity measurement at the transducer head was used to collect multibeam data. Patch tests were performed to calibrate the inertial navigation system. Sound velocity profiles were measured to correct echosounder data for stratification with depth. The multibeam data were processed to include corrections for sound velocity, conversion of depth to elevation using a time series of water surface elevation, and to remove erroneous points. Following multibeam data processing and editing, almost 3.7 billion point observations remained. Multibeam echosounder data, ADCP data, and lidar data were combined to create 3.28-foot raster grids for each lake. Estimated points were used to represent unmeasurable areas (for example, near structures and islands) in the grids. Grid cells with no data from these sources were interpolated from surrounding data, and additional estimated points were used to improve the interpolation of bathymetric surfaces. Bathymetric contours at 2-foot intervals of elevation and elevation-area-capacity tables were computed from the raster grid. The geospatial bathymetric data and results are available as a USGS data release.

The results of the bathymetric survey indicate that New York City's EOH reservoirs and controlled lakes are between about 25 and more than 160 feet deep and have a total capacity of about 142.9 billion gallons at full spillway level and a combined surface area of more than 11,600 acres. The accuracy of the mapped raster grids was evaluated using a quality assurance dataset collected with a single-beam echosounder; about 280,000 quality assurance points were spatially joined with the mapped raster surfaces in a geographic information system, and the measured elevations were compared. The calculated mean elevation error for the East of Hudson reservoirs was 0.35 foot, the median error was 0.21 foot, and the 95-percent accuracy was 1.68 feet; the 95-percent accuracy of the computed capacity at spillway elevation was 1.6 percent or less.

References Cited

AML Oceanographic, 2010, Smart SV user manual (ver. 2.1, January 13, 2010): AML Oceanographic, 22 p., accessed October 26, 2020, at https://amloceanographic.com/documents/#1147-1130-wpfd-traditional-instruments.

Applanix Corp., 2017, POS MV V5 installation and operation guide, rev. 17: Richmond Hill, Ontario, Canada, Applanix Corp. PUBS–MAN–004291, 293 p., accessed October 5, 2016, at https://amloceanographic.app.boxenterprise.net/web_links/3328063/shared/a1qjym370915odho0683.

Esri Inc., 2020, ArcGIS Desktop: Esri Inc. software, accessed October 27, 2020, at https://www.esri.com/en-us/arcgis/products/arcgis-desktop/overview.

Federal Geographic Data Committee, 1998, National standard for spatial data accuracy, pt. 3 *of* Geospatial positioning accuracy standards: Federal Geographic Data Committee FGDC–STD–007.3, p. 3–1—3–25, accessed February 14, 2021, at https://www.fgdc.gov/standards/projects/accuracy/part3/chapter3.

Helsel, D.R., Hirsch, R.M., Ryberg, K.R., Archfield, S.A., and Gilroy, E.J., 2020, Statistical methods in water resources: U.S. Geological Survey Techniques and Methods, book 4, chap. A3, 458 p., accessed June 23, 2020, at https://doi.org/10.3133/tm4a3.

Hemisphere, G.N.S.S., Inc., 2017, V102 GPS Compass user guide: Hemisphere GNSS, Inc. Part 875–0276–000 Rev C2, 60 p., accessed February 14, 2021, at https://www.hemispheregnss.com/wp-content/uploads/2018/12/hemispheregnss_v102_userguide_875-0276-000_c2-1.pdf.

Huizinga, R.J., 2016, Bathymetric and velocimetric surveys at highway bridges crossing the Missouri River near Kansas City, Missouri, June 2–4, 2015: U.S. Geological Survey Scientific Investigations Report 2016–5061, 93 p., accessed June 23, 2020, at https://doi.org/10.3133/sir20165061.

Huizinga, R.J., and Heimann, D.C., 2018, Hydrographic surveys of rivers and lakes using a multibeam echosounder mapping system: U.S. Geological Survey Fact Sheet 2018–3021, 6 p., accessed June 23, 2020, at https://doi.org/10.3133/fs20183021.

HYPACK, 2021, New releases & program updates: HYPACK web page, accessed February 14, 2021, at https://www.hypack.com/customer-support/programs-and-updates.

National Marine Electronics Association, 2002, Standard for interfacing marine electronic devices (ver. 3.01): National Marine Electronics Association standard NMEA 0183, 88 p., accessed June 23, 2020, at https://www.plaisance-pratique.com/IMG/pdf/NMEA0183-2.pdf.

New York City Department of Environmental Protection (NYCDEP), 2009, East of Hudson lidar data: New York City Department of Environmental Protection data, accessed March 24, 2020, at ftp://ftp.gis.ny.gov/elevation/LIDAR/NYCDEP_EastOfHudson2009/2009_EOH.xml.

New York City Department of Environmental Protection (NYCDEP), 2020a, History of New York City drinking water: New York City Department of Environmental Protection web page, accessed October 6, 2020, at https://www1.nyc.gov/site/dep/water/history-of-new-york-citys-drinking-water.page.

New York City Department of Environmental Protection (NYCDEP), 2020b, New York City drinking water supply and quality report—2019: New York City Department of Environmental Protection, 20 p., accessed October 6, 2020, at https://www1.nyc.gov/assets/dep/downloads/pdf/water/drinking-water/drinking-water-supply-quality-report/2019-drinking-water-supply-quality-report.pdf.

New York City Department of Environmental Protection (NYCDEP), 2021a, Amawalk Reservoir: New York City Department of Environmental Protection web page, accessed February 14, 2021, at https://www1.nyc.gov/site/dep/water/amawalk-reservoir.page.

New York City Department of Environmental Protection (NYCDEP), 2021b, Bog Brook Reservoir: New York City Department of Environmental Protection web page, accessed February 14, 2021, at https://www1.nyc.gov/site/dep/water/bog-brook-reservoir.page.

New York City Department of Environmental Protection (NYCDEP), 2021c, Boyd Corners Reservoir: New York City Department of Environmental Protection web page, accessed February 14, 2021, at https://www1.nyc.gov/site/dep/water/boyds-corner-reservoir.page.

New York City Department of Environmental Protection (NYCDEP), 2021d, Cross River Reservoir: New York City Department of Environmental Protection web page, accessed February 14, 2021, at https://www1.nyc.gov/site/dep/water/cross-river-reservoir.page.

New York City Department of Environmental Protection (NYCDEP), 2021e, Croton Falls Reservoir: New York City Department of Environmental Protection web page, accessed February 14, 2021, at https://www1.nyc.gov/site/dep/water/croton-falls-reservoir.page.

New York City Department of Environmental Protection (NYCDEP), 2021f, Diverting Reservoir: New York City Department of Environmental Protection web page, accessed February 14, 2021, at https://www1.nyc.gov/site/dep/water/diverting-reservoir.page.

New York City Department of Environmental Protection (NYCDEP), 2021g, East Branch Reservoir: New York City Department of Environmental Protection web page, accessed February 14, 2021, at https://www1.nyc.gov/site/dep/water/east-branch-reservoir.page.

New York City Department of Environmental Protection (NYCDEP), 2021h, Kensico Reservoir: New York City Department of Environmental Protection web page, accessed February 14, 2021, at https://www1.nyc.gov/site/dep/water/kensico-reservoir.page.

New York City Department of Environmental Protection (NYCDEP), 2021i, Middle Branch Reservoir: New York City Department of Environmental Protection web page, accessed February 14, 2021, at https://www1.nyc.gov/site/dep/water/middle-branch-reservoir.page.

New York City Department of Environmental Protection (NYCDEP), 2021j, Muscoot Reservoir: New York City Department of Environmental Protection web page, accessed February 14, 2021, at https://www1.nyc.gov/site/dep/water/muscoot-reservoir.page.

New York City Department of Environmental Protection (NYCDEP), 2021k, New Croton Reservoir: New York City Department of Environmental Protection web page, accessed February 14, 2021, at https://www1.nyc.gov/site/dep/water/new-croton-reservoir.page.

New York City Department of Environmental Protection (NYCDEP), 2021l, Titicus Reservoir: New York City Department of Environmental Protection web page, accessed February 14, 2021, at https://www1.nyc.gov/site/dep/water/titicus-reservoir.page.

New York City Department of Environmental Protection (NYCDEP), 2021m, West Branch Reservoir: New York City Department of Environmental Protection web page, accessed February 14, 2021, at https://www1.nyc.gov/site/dep/water/west-branch-reservoir.page.

New York State Department of Transportation, 2021, NYSNet spatial reference network (CORS/real time network): New York State Department of Transportation web page, accessed February 9, 2021, at https://www.dot.ny.gov/divisions/engineering/design/design-services/land-survey/cors.

Nystrom, E.A., 2018, Bathymetry of Ashokan, Cannonsville, Neversink, Pepacton, Rondout, and Schoharie reservoirs, New York, 2013–15: U.S. Geological Survey Scientific Investigations Report 2017–5064, 29 p., accessed June 23, 2020, at https://doi.org/10.3133/sir20175064.

Nystrom, E.A., and Collenburg, J.V., 2020, Bathymetry of Morris Lake (Newton Reservoir), New Jersey, 2018: U.S. Geological Survey Scientific Investigations Report 2020–5010, 14 p., accessed June 23, 2020, at https://doi.org/10.3133/sir20205010.

Nystrom, E.A., Huston, C.J., and Welk, R.J., 2021, Geospatial bathymetry datasets for New York City's East of Hudson reservoirs and controlled lakes: U.S. Geological Survey data release, https://doi.org/10.5066/P9ZZQ2OT.

SyQwest, Inc., 2008, Bathy-500MF multi frequency-survey echosounder: SyQwest, Inc. installation, operation, and maintenance manual, 58 p., accessed February 14, 2021, at https://www.syqwestinc.com/media/bathy-500mf/bathy500mf-manual.pdf.

Teledyne Marine, 2016, Introducing RioPro—Your Rio Grande upgrade path: Teledyne Marine news, September 1, 2016, accessed February 10, 2021, at http://www.teledynemarine.com/news/RDI_RioPro_Upgrade.

Teledyne Marine, 2020, WinRiver II software user's guide: Teledyne Marine, 318 p., accessed March 3, 2021, at http://www.teledynemarine.com/Documents/Brand%20Support/RD%20INSTRUMENTS/Technical%20Resources/Manuals%20and%20Guides/Workhorse/WinRiver%20II%20User%20Guide_Mar20.pdf.

Teledyne Marine Odom Hydrographic, 2021, MB2 multibeam echosounder: Teledyne Marine Odom Hydrographic product datasheet, 2 p., accessed February 14, 2021, at http://www.teledynemarine.com/Lists/Downloads/Odom/Teledyne%20Odom%20MB2%20product%20leaflet.pdf.

Teledyne PDS, 2019, Teledyne PDS version 4.3.12: Teledyne PDS user manual, 869 p., accessed March 2, 2021, at http://www.teledynemarine.com/Lists/Downloads/PDS%20leaflets%20and%20manuels/PDS%20Manuals/Teledyne%20PDS%20User%20Manual.pdf.

Teledyne PDS, 2021a, Multibeam survey and processing/charting: Teledyne PDS leaflet, 2 p., accessed February 14, 2021, at http://www.teledynemarine.com/Lists/Downloads/PDS%20leaflets%20and%20manuels/Multibeam%20Survey%20and%20Processing-Charting_product%20leaflet.pdf.

Teledyne PDS, 2021b, PDS multibeam survey and processing/charting: Teledyne PDS web page, accessed May 5, 2021, at http://www.teledynemarine.com/pds-multibeam-survey-and-processing-charting.

Teledyne RESON, 2021, SVP 70—Fixed-mount sound velocity probe: Teledyne RESON product leaflet, 2 p., accessed February 14, 2021, at http://www.teledynemarine.com/Lists/Downloads/SVP_70_%20product%20leaflet.pdf.

Trimble Inc., 2009, Trimble R8 GNSS receiver Trimble R6/5800 GPS receiver: Trimble Inc. user guide, 86 p., accessed February 14, 2021, at http://trl.trimble.com/docushare/dsweb/Get/Document-666215/R8-R6-5800_v400A_UserGuide.pdf.

Trimble Inc., 2021, Trimble Business Center—Office software for surveyors: Trimble Inc. web page, accessed February 14, 2021, at https://geospatial.trimble.com/products-and-solutions/trimble-business-center.

Wilson, G.L., and Richards, J.M., 2006, Procedural documentation and accuracy assessment of bathymetric maps and area/capacity tables for small reservoirs: U.S. Geological Survey Scientific Investigations Report 2006–5208, 24 p., oversized figs., accessed June 23, 2020, at https://doi.org/10.3133/sir20065208.

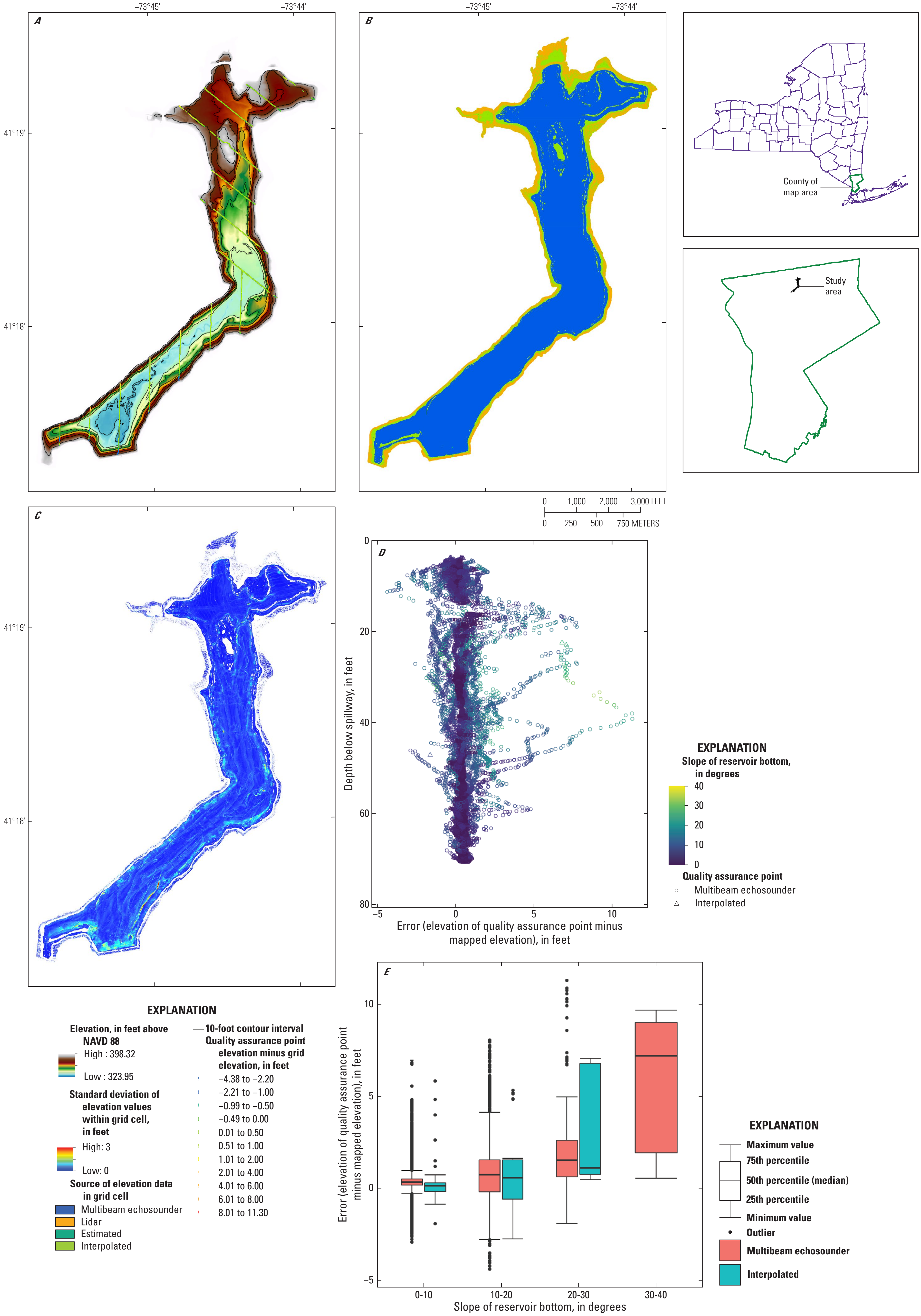

Figure 10. Results of bathymetric mapping of Amawalk Reservoir in Westchester County, New York, including maps of *A*, bathymetric elevations, contours, and quality assurance points, *B*, source data type, and *C*, cell standard deviation; and plots showing comparison of quality assurance points and mapped elevation *D*, by depth and slope and *E*, by grid cell data source. Mapped data are from Nystrom and others (2021). Lidar, light detection and ranging; NAVD 88; North American Vertical Datum of 1988. A large version of this figure is available for download at https://doi.org/10.3133/sir20215057.

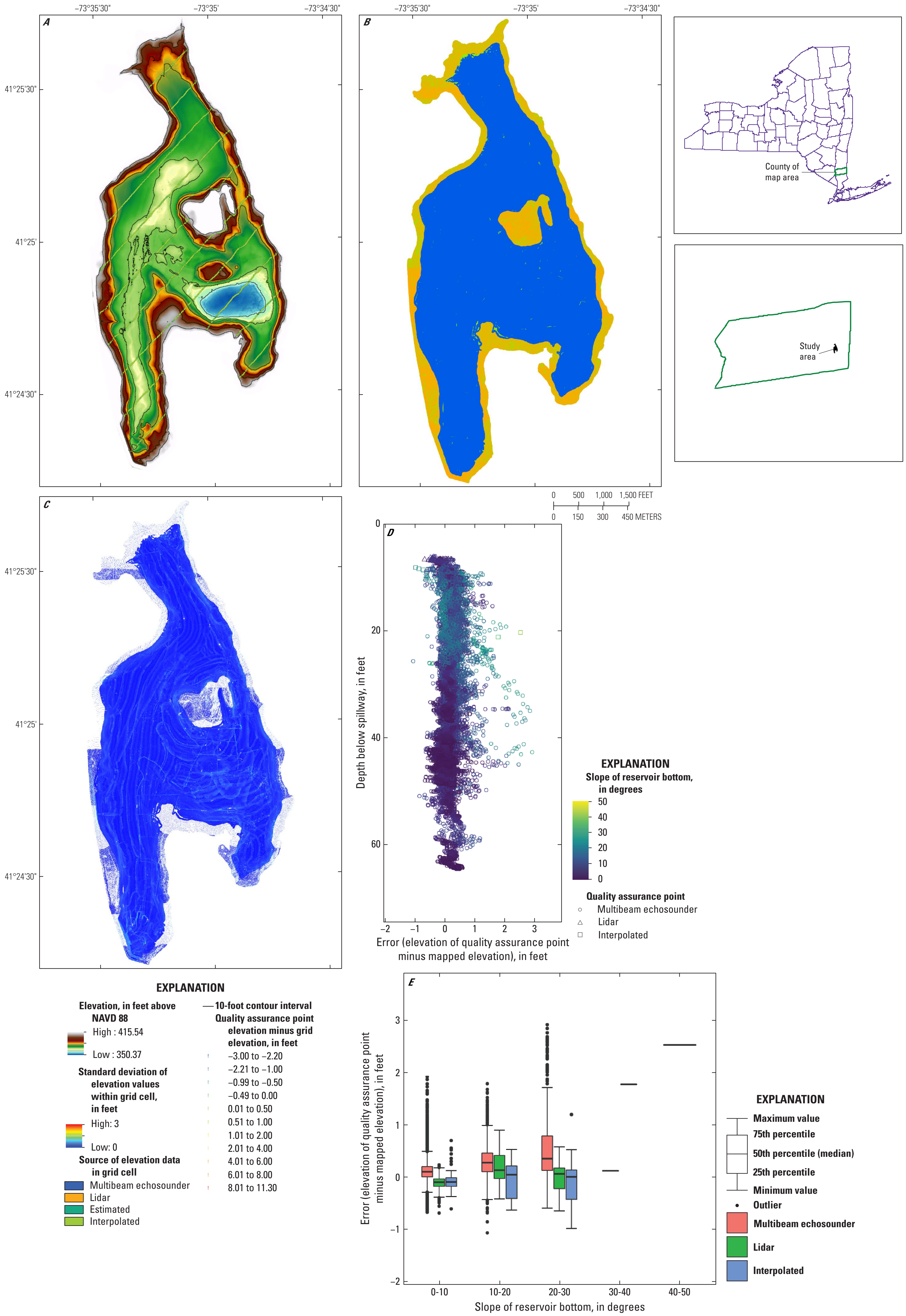

Figure 11. Results of bathymetric mapping of Bog Brook Reservoir in Putnam County, New York, including maps of *A*, bathymetric elevations, contours, and quality assurance points, *B*, source data type, and *C*, cell standard deviation; and plots showing comparison of quality assurance points and mapped elevation *D*, by depth and slope and *E*, by grid cell data source. Mapped data are from Nystrom and others (2021). Lidar, light detection and ranging; NAVD 88; North American Vertical Datum of 1988. A large version of this figure is available for download at https://doi.org/10.3133/sir20215057.

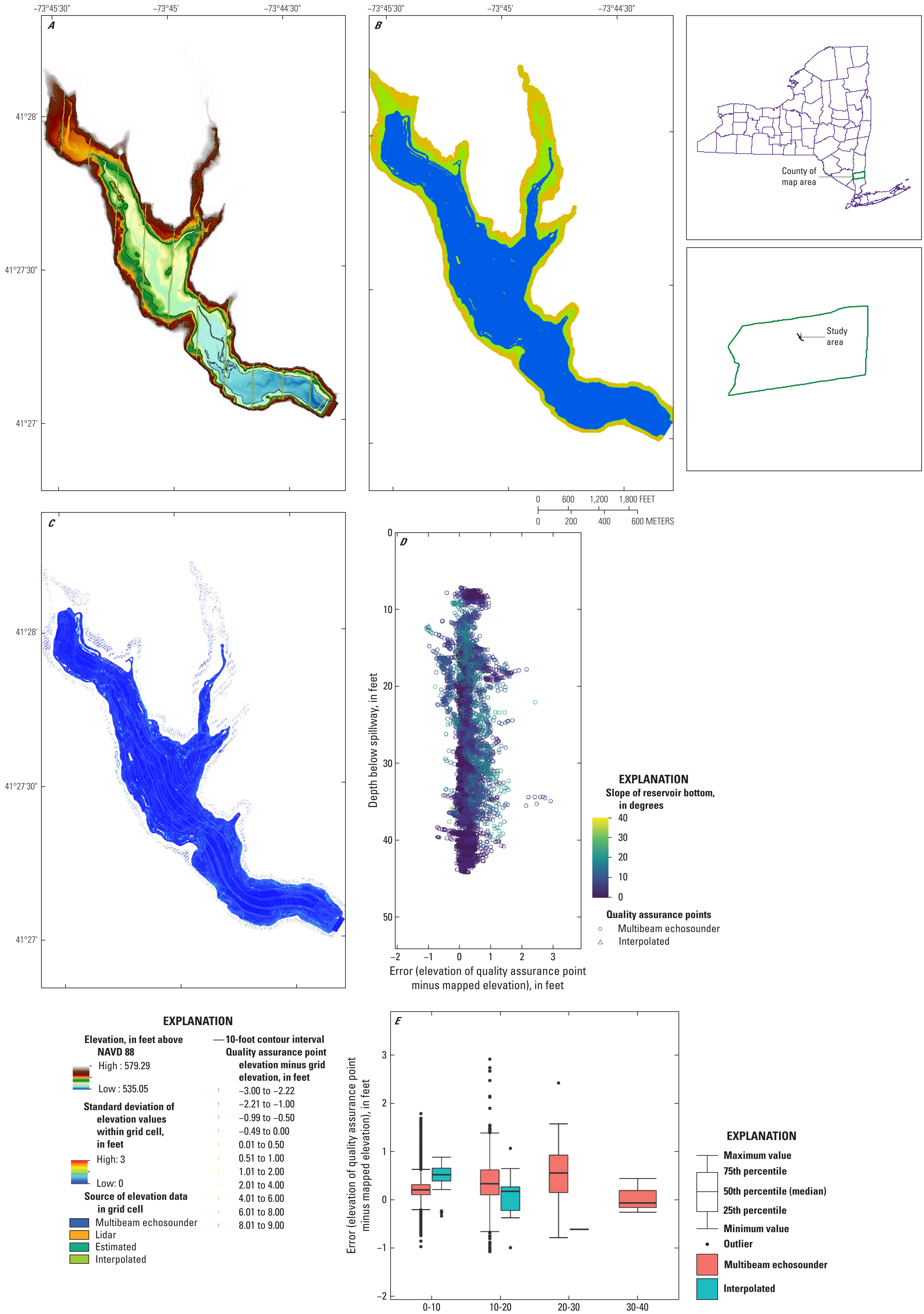

Figure 12. Results of bathymetric mapping of Boyd Corners Reservoir in Putnam County, New York, including maps of *A*, bathymetric elevations, contours, and quality assurance points, *B*, source data type, and *C*, cell standard deviation; and plots showing comparison of quality assurance points and mapped elevation *D*, by depth and slope and *E*, by grid cell data source. Mapped data are from Nystrom and others (2021). Lidar, light detection and ranging; NAVD 88; North American Vertical Datum of 1988. A large version of this figure is available for download at https://doi.org/10.3133/sir20215057.

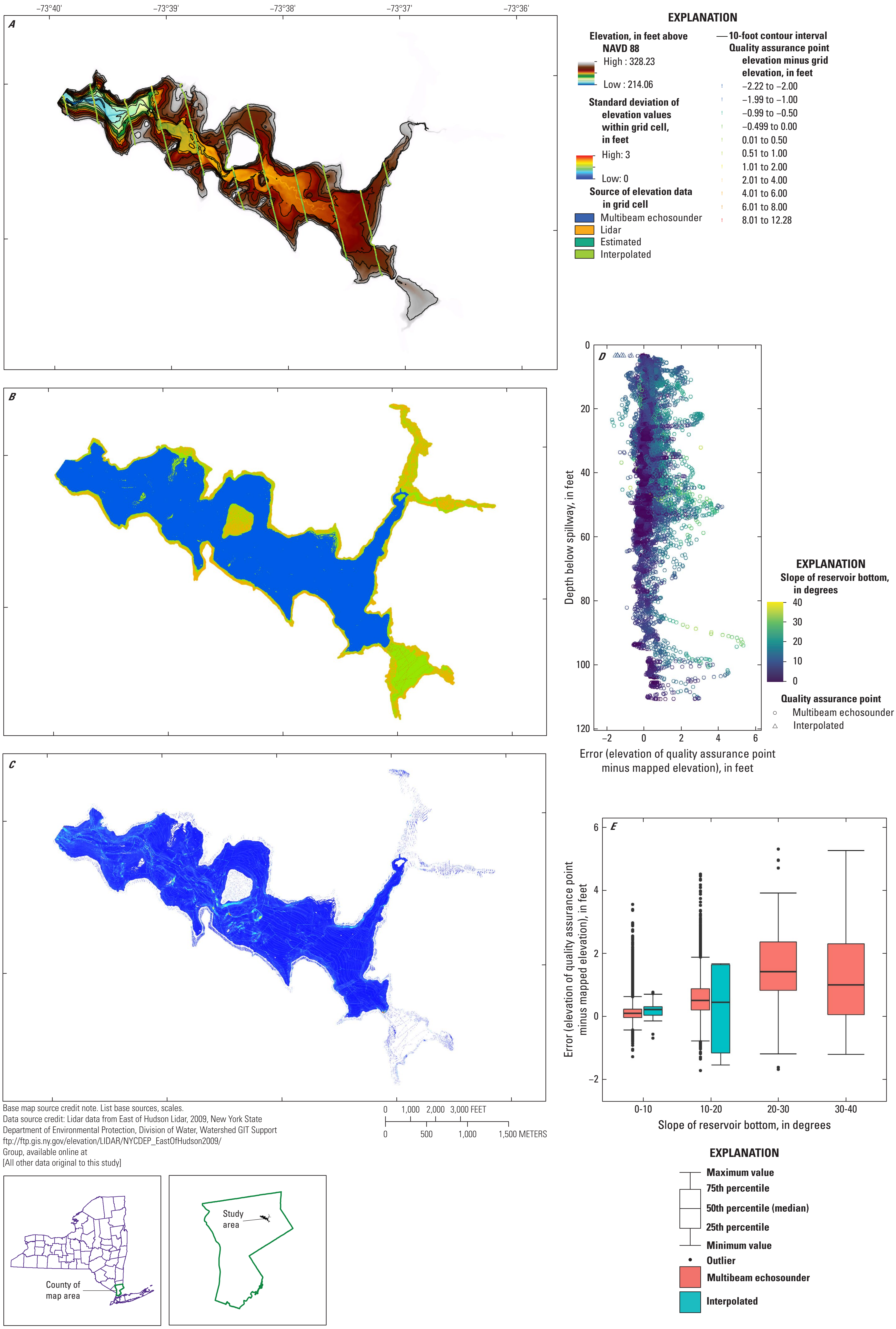

Figure 13. Results of bathymetric mapping of Cross River Reservoir in Westchester County, New York, including maps of *A*, bathymetric elevations, contours, and quality assurance points, *B*, source data type, and *C*, cell standard deviation; and plots showing comparison of quality assurance points and mapped elevation *D*, by depth and slope and *E*, by grid cell data source. Mapped data are from Nystrom and others (2021). Lidar, light detection and ranging; NAVD 88; North American Vertical Datum of 1988. A large version of this figure is available for download at https://doi.org/10.3133/sir20215057.

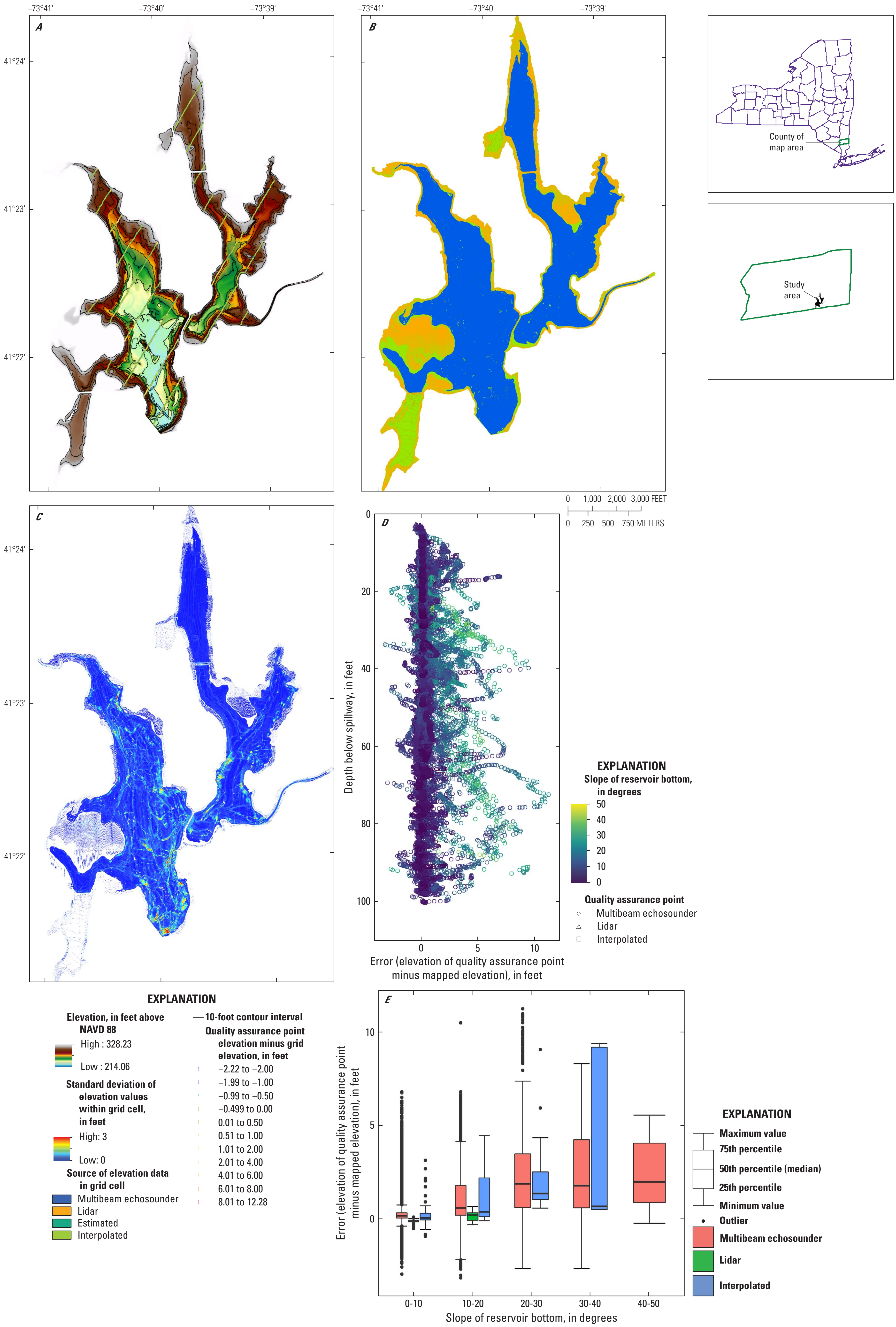

Figure 14. Results of bathymetric mapping of Croton Falls Reservoir in Putnam County, New York, including maps of *A*, bathymetric elevations, contours, and quality assurance points, *B*, source data type, and *C*, cell standard deviation; and plots showing comparison of quality assurance points and mapped elevation *D*, by depth and slope and *E*, by grid cell data source. Mapped data are from Nystrom and others (2021). Lidar, light detection and ranging; NAVD 88; North American Vertical Datum of 1988. A large version of this figure is available for download at https://doi.org/10.3133/sir20215057.

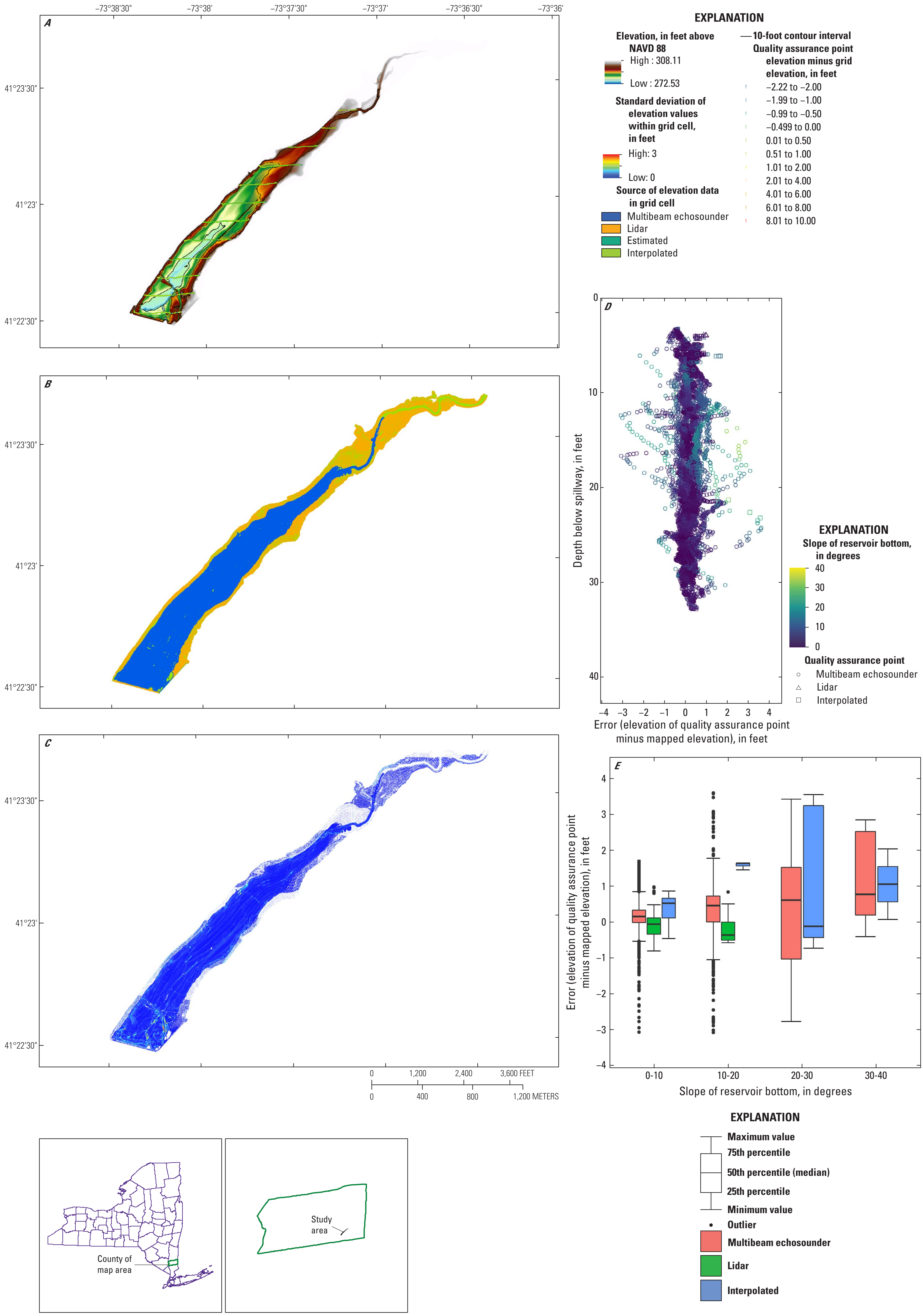

Figure 15. Results of bathymetric mapping of Diverting Reservoir in Putnam County, New York, including maps of *A*, bathymetric elevations, contours, and quality assurance points, *B*, source data type, and *C*, cell standard deviation; and plots showing comparison of quality assurance points and mapped elevation *D*, by depth and slope and *E*, by grid cell data source. Mapped data are from Nystrom and others (2021). Lidar, light detection and ranging; NAVD 88; North American Vertical Datum of 1988. A large version of this figure is available for download at https://doi.org/10.3133/sir20215057.

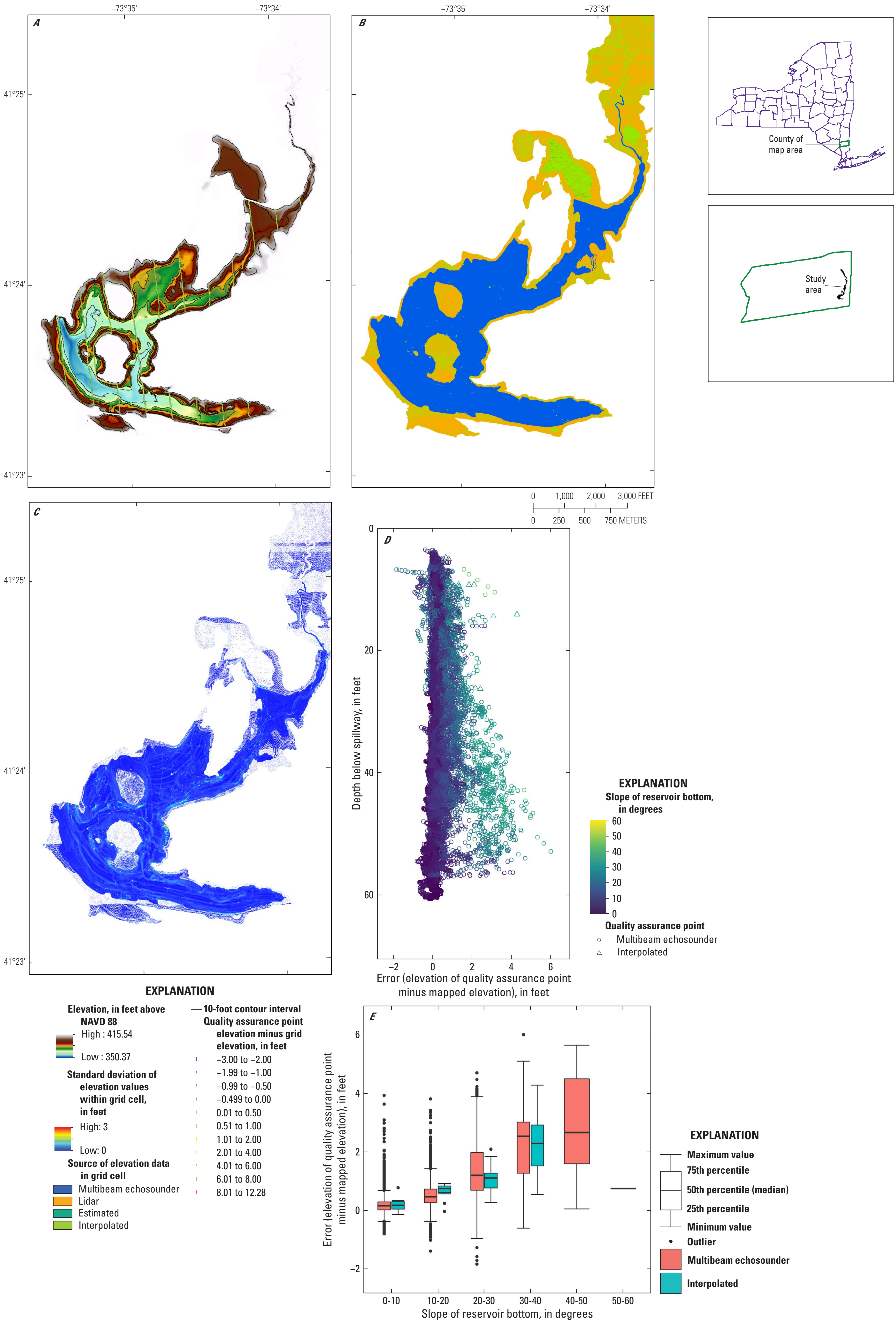

Figure 16. Results of bathymetric mapping of East Branch Reservoir in Putnam County, New York, including maps of *A*, bathymetric elevations, contours, and quality assurance points, *B*, source data type, and *C*, cell standard deviation; and plots showing comparison of quality assurance points and mapped elevation *D*, by depth and slope and *E*, by grid cell data source. Mapped data are from Nystrom and others (2021). Lidar, light detection and ranging; NAVD 88; North American Vertical Datum of 1988. A large version of this figure is available for download at https://doi.org/10.3133/sir20215057.

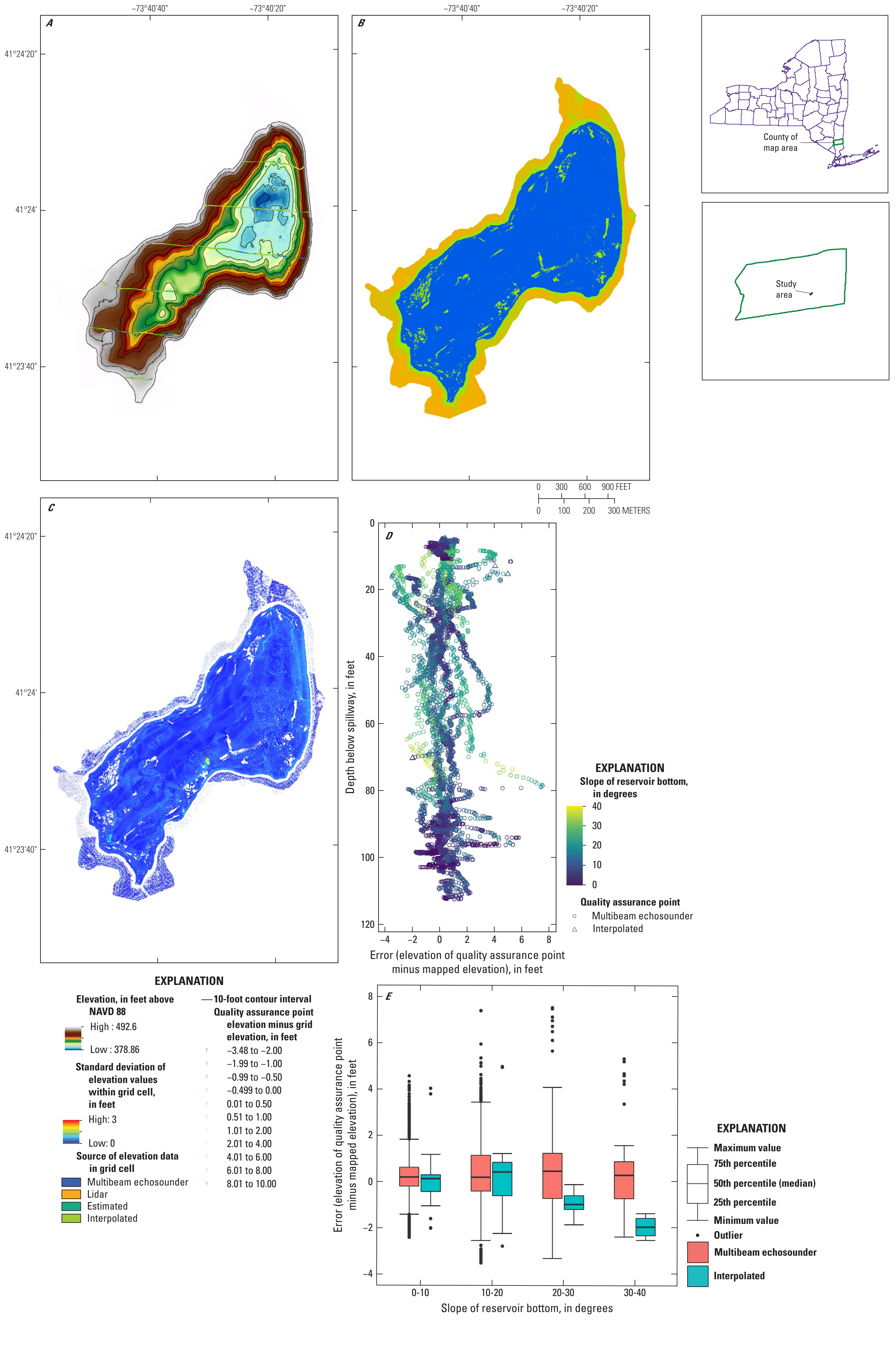

Figure 17. Results of bathymetric mapping of Lake Gilead in Putnam County, New York, including maps of *A*, bathymetric elevations, contours, and quality assurance points, *B*, source data type, and *C*, cell standard deviation; and plots showing comparison of quality assurance points and mapped elevation *D*, by depth and slope and *E*, by grid cell data source. Mapped data are from Nystrom and others (2021). Lidar, light detection and ranging; NAVD 88; North American Vertical Datum of 1988. A large version of this figure is available for download at https://doi.org/10.3133/sir20215057.

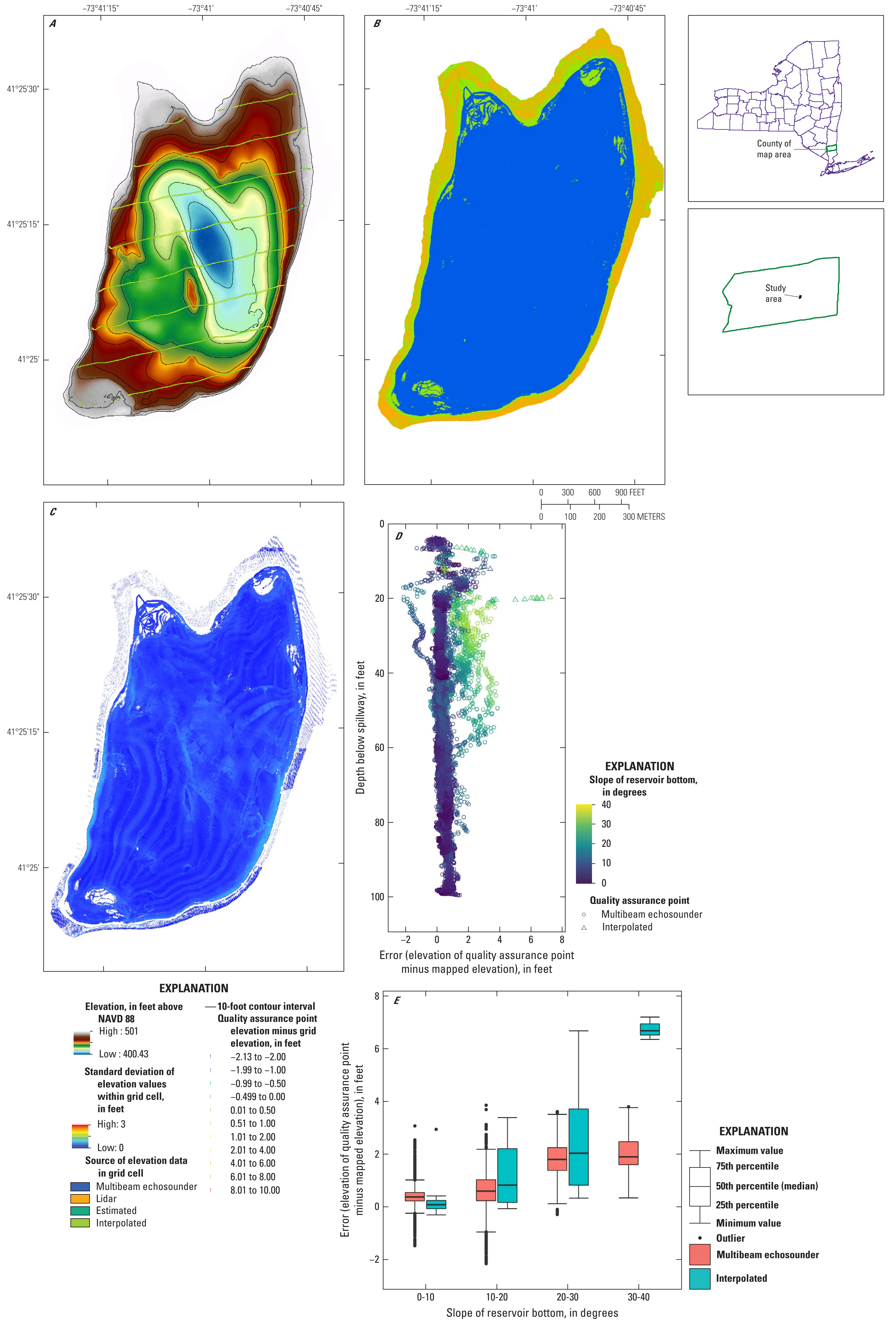

Figure 18. Results of bathymetric mapping of Lake Gleneida in Putnam County, New York, including maps of *A*, bathymetric elevations, contours, and quality assurance points, *B*, source data type, and *C*, cell standard deviation; and plots showing comparison of quality assurance points and mapped elevation *D*, by depth and slope and *E*, by grid cell data source. Mapped data are from Nystrom and others (2021). Lidar, light detection and ranging; NAVD 88; North American Vertical Datum of 1988. A large version of this figure is available for download at https://doi.org/10.3133/sir20215057.

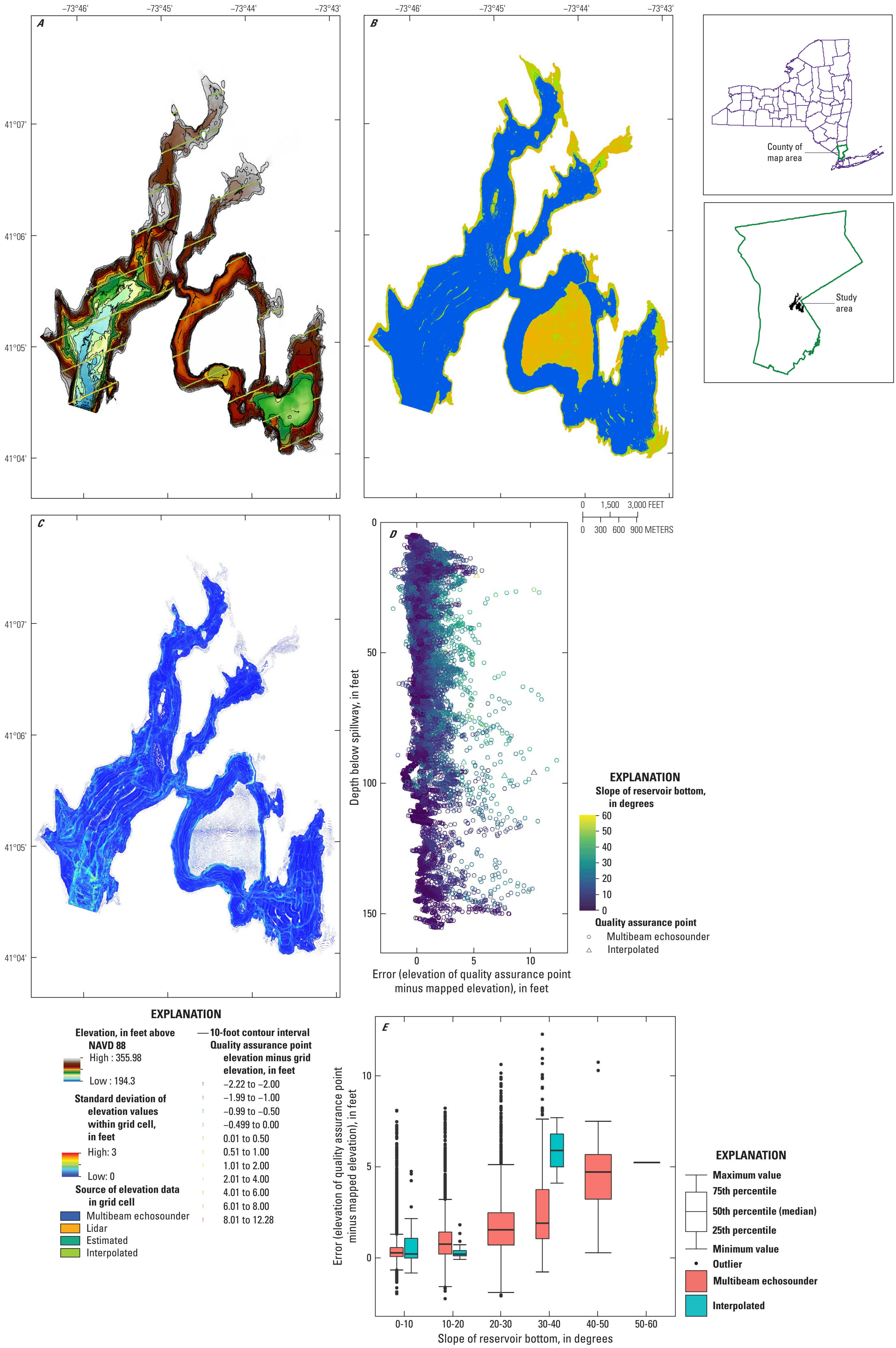

Figure 19. Results of bathymetric mapping of Kensico Reservoir in Westchester County, New York, including maps of *A*, bathymetric elevations, contours, and quality assurance points, *B*, source data type, and *C*, cell standard deviation; and plots showing comparison of quality assurance points and mapped elevation *D*, by depth and slope and *E*, by grid cell data source. Mapped data are from Nystrom and others (2021). Lidar, light detection and ranging; NAVD 88; North American Vertical Datum of 1988. A large version of this figure is available for download at https://doi.org/10.3133/sir20215057.

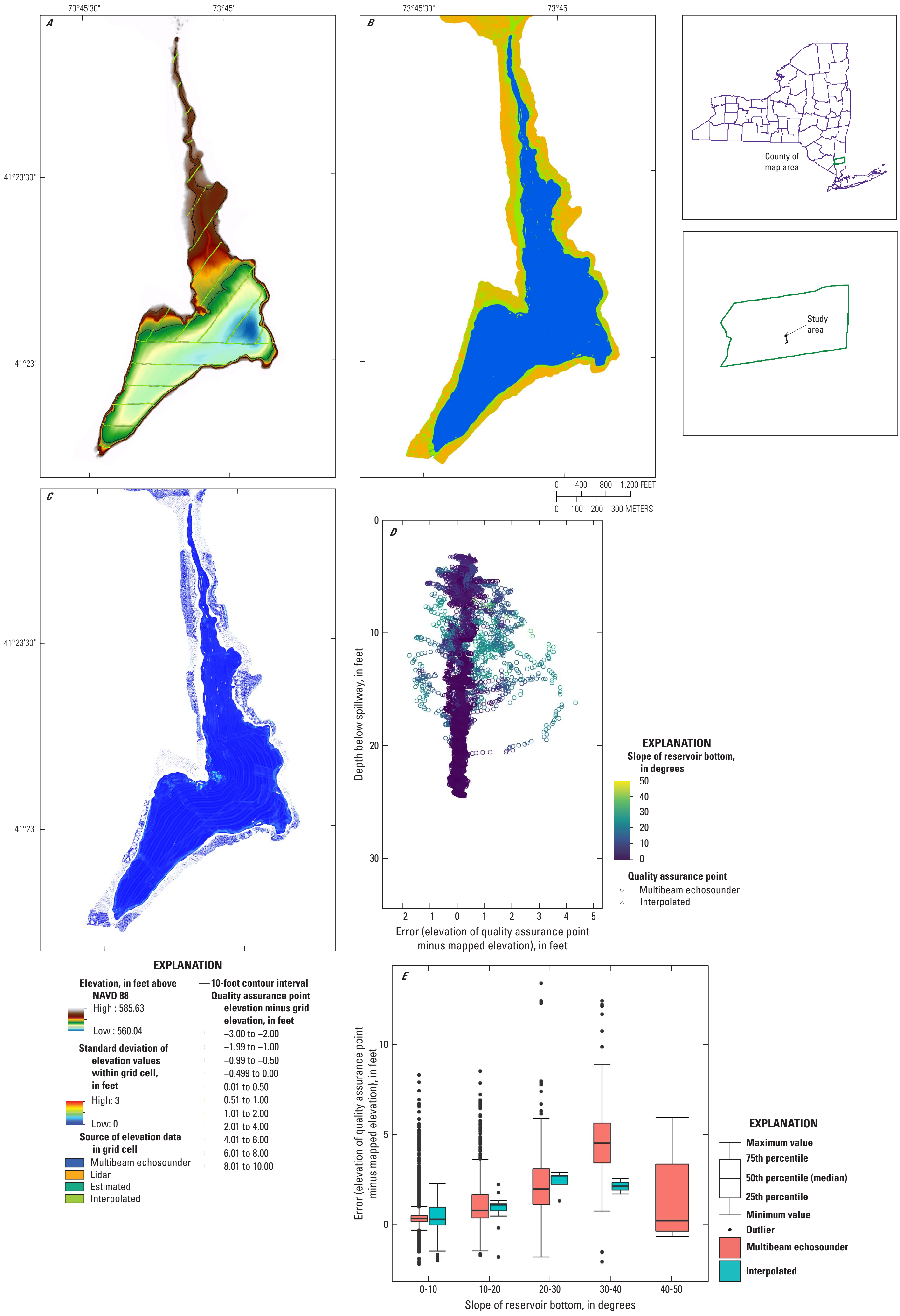

Figure 20. Results of bathymetric mapping of Kirk Lake in Putnam County, New York, including maps of *A*, bathymetric elevations, contours, and quality assurance points, *B*, source data type, and *C*, cell standard deviation; and plots showing comparison of quality assurance points and mapped elevation *D*, by depth and slope and *E*, by grid cell data source. Mapped data are from Nystrom and others (2021). Lidar, light detection and ranging; NAVD 88; North American Vertical Datum of 1988. A large version of this figure is available for download at https://doi.org/10.3133/sir20215057.

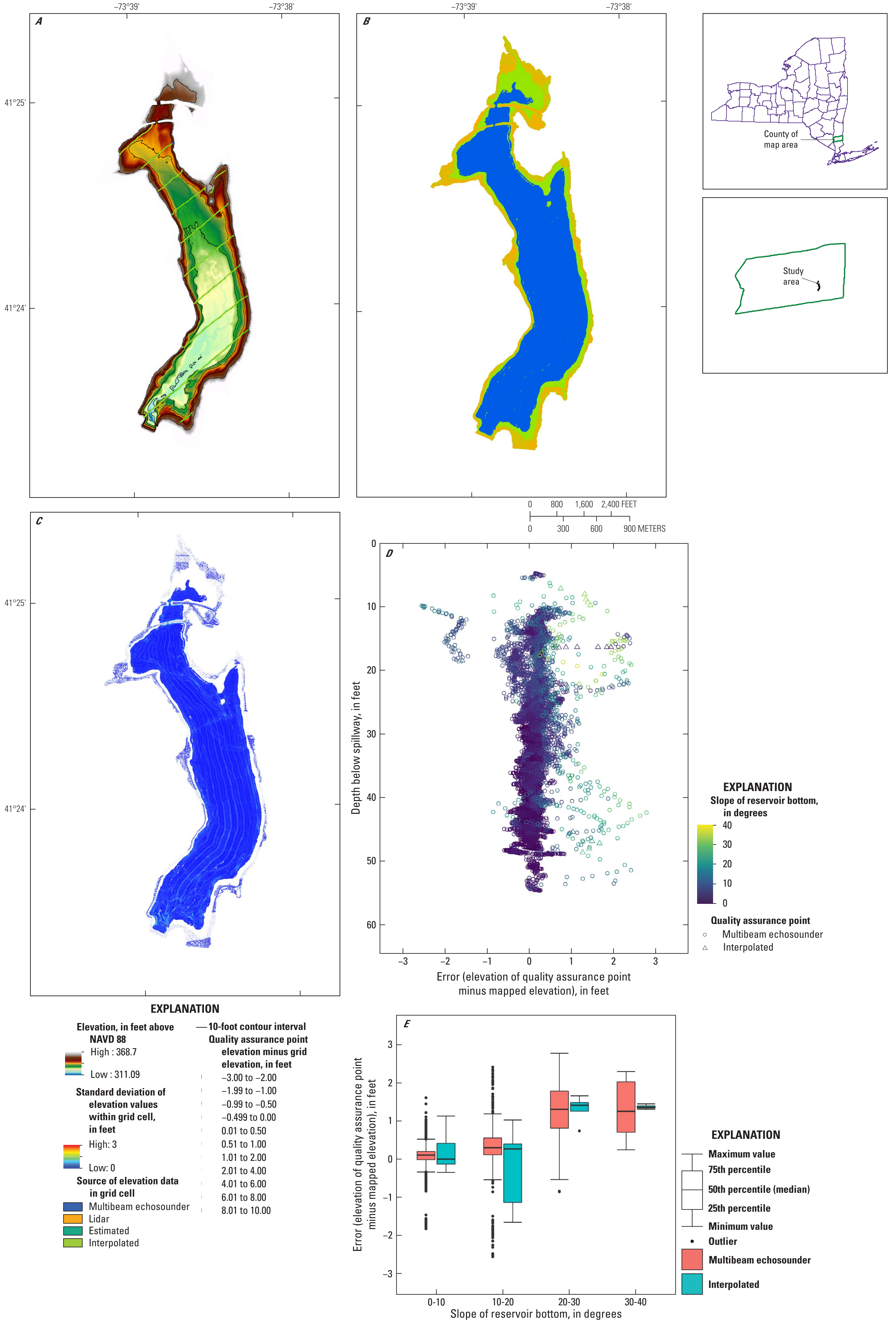

Figure 21. Results of bathymetric mapping of Middle Branch Reservoir in Putnam County, New York, including maps of *A*, bathymetric elevations, contours, and quality assurance points, *B*, source data type, and *C*, cell standard deviation; and plots showing comparison of quality assurance points and mapped elevation *D*, by depth and slope and *E*, by grid cell data source. Mapped data are from Nystrom and others (2021). Lidar, light detection and ranging; NAVD 88; North American Vertical Datum of 1988. A large version of this figure is available for download at https://doi.org/10.3133/sir20215057.

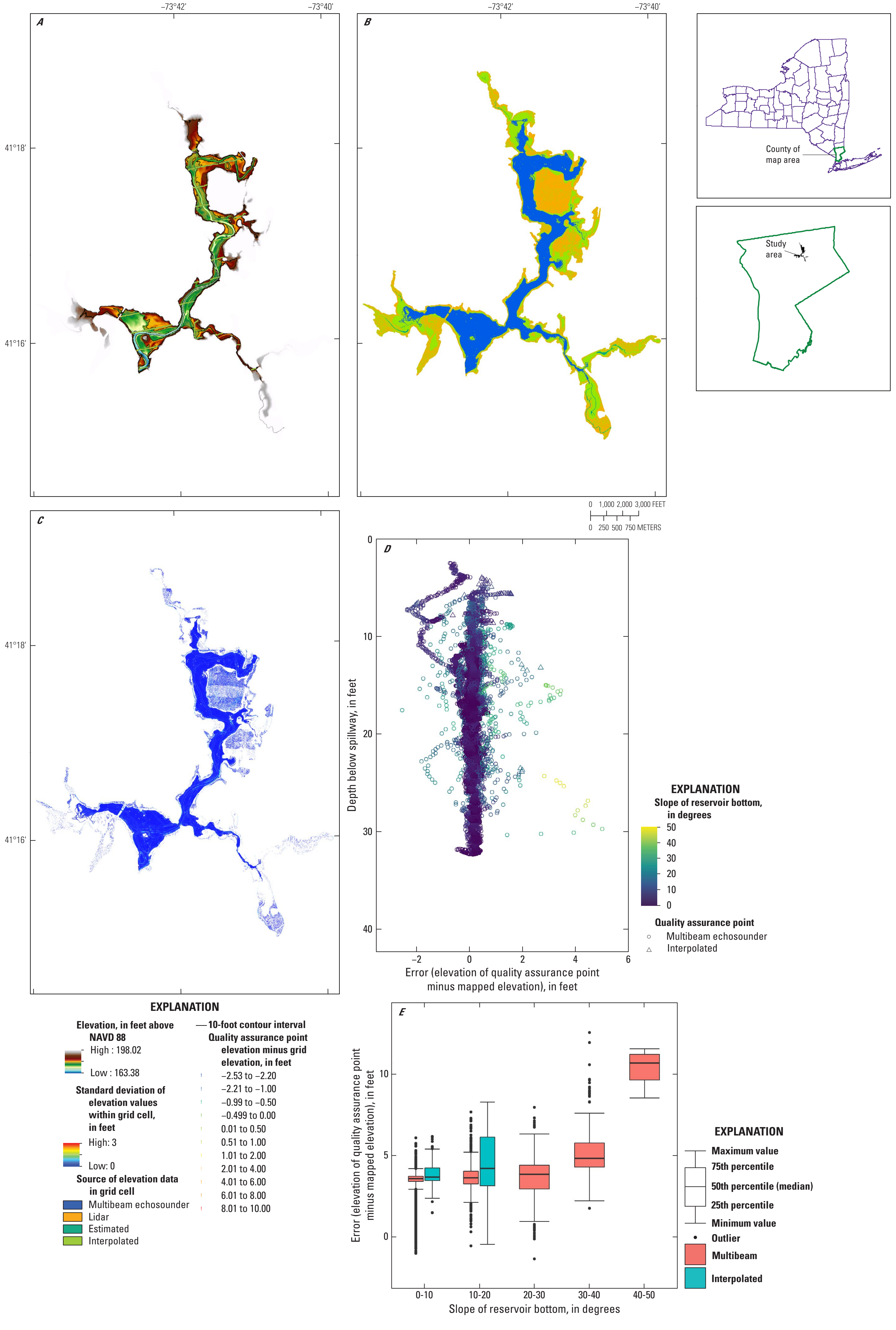

Figure 22. Results of bathymetric mapping of Muscoot Reservoir in Westchester County, New York, including maps of *A*, bathymetric elevations, contours, and quality assurance points, *B*, source data type, and *C*, cell standard deviation; and plots showing comparison of quality assurance points and mapped elevation *D*, by depth and slope and *E*, by grid cell data source. Mapped data are from Nystrom and others (2021). Lidar, light detection and ranging; NAVD 88; North American Vertical Datum of 1988. A large version of this figure is available for download at https://doi.org/10.3133/sir20215057.

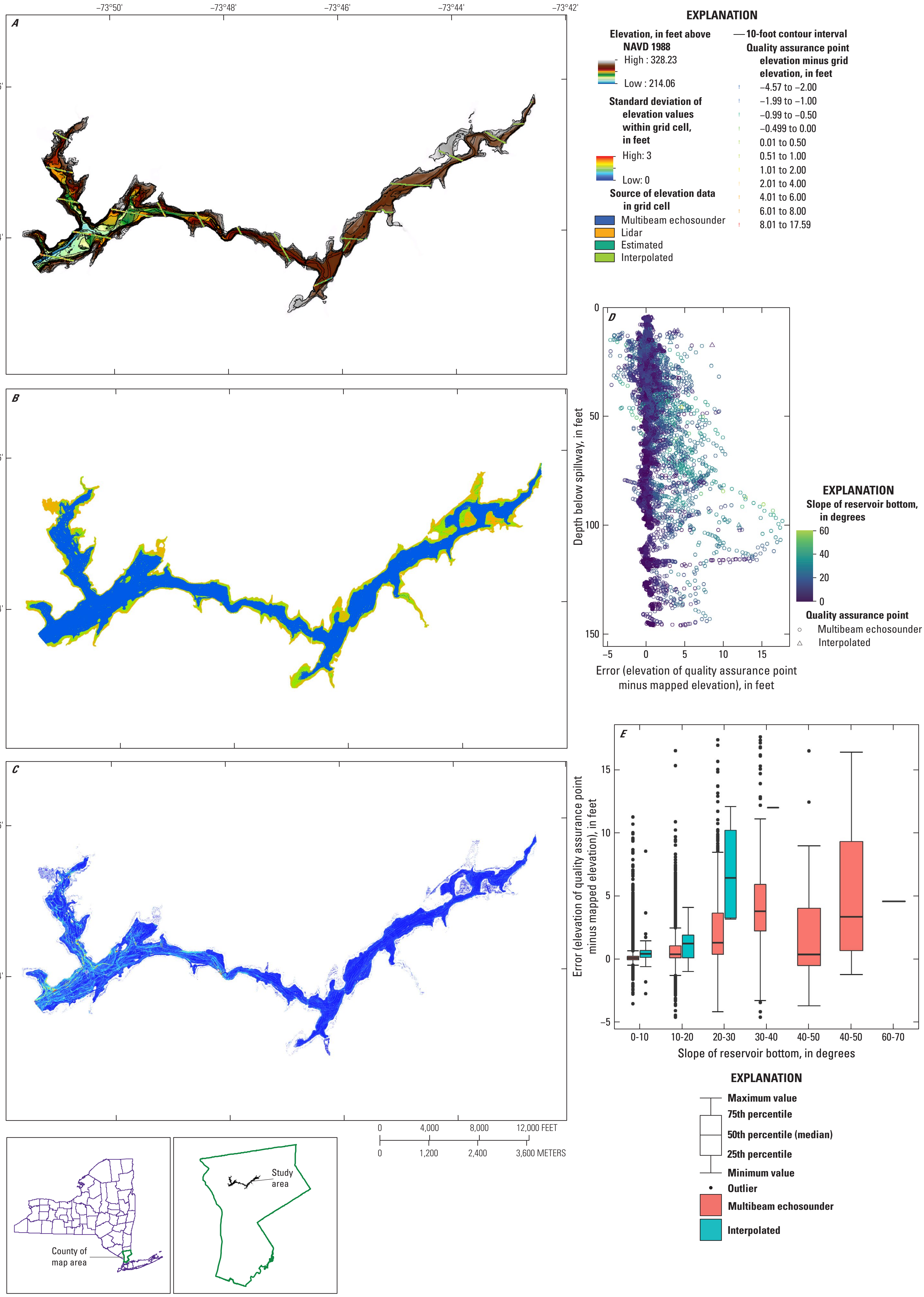

Figure 23. Results of bathymetric mapping of New Croton Reservoir in Westchester County, New York, including maps of *A*, bathymetric elevations, contours, and quality assurance points, *B*, source data type, and *C*, cell standard deviation; and plots showing comparison of quality assurance points and mapped elevation *D*, by depth and slope and *E*, by grid cell data source. Mapped data are from Nystrom and others (2021). Lidar, light detection and ranging; NAVD 88; North American Vertical Datum of 1988. A large version of this figure is available for download at https://doi.org/10.3133/sir20215057.

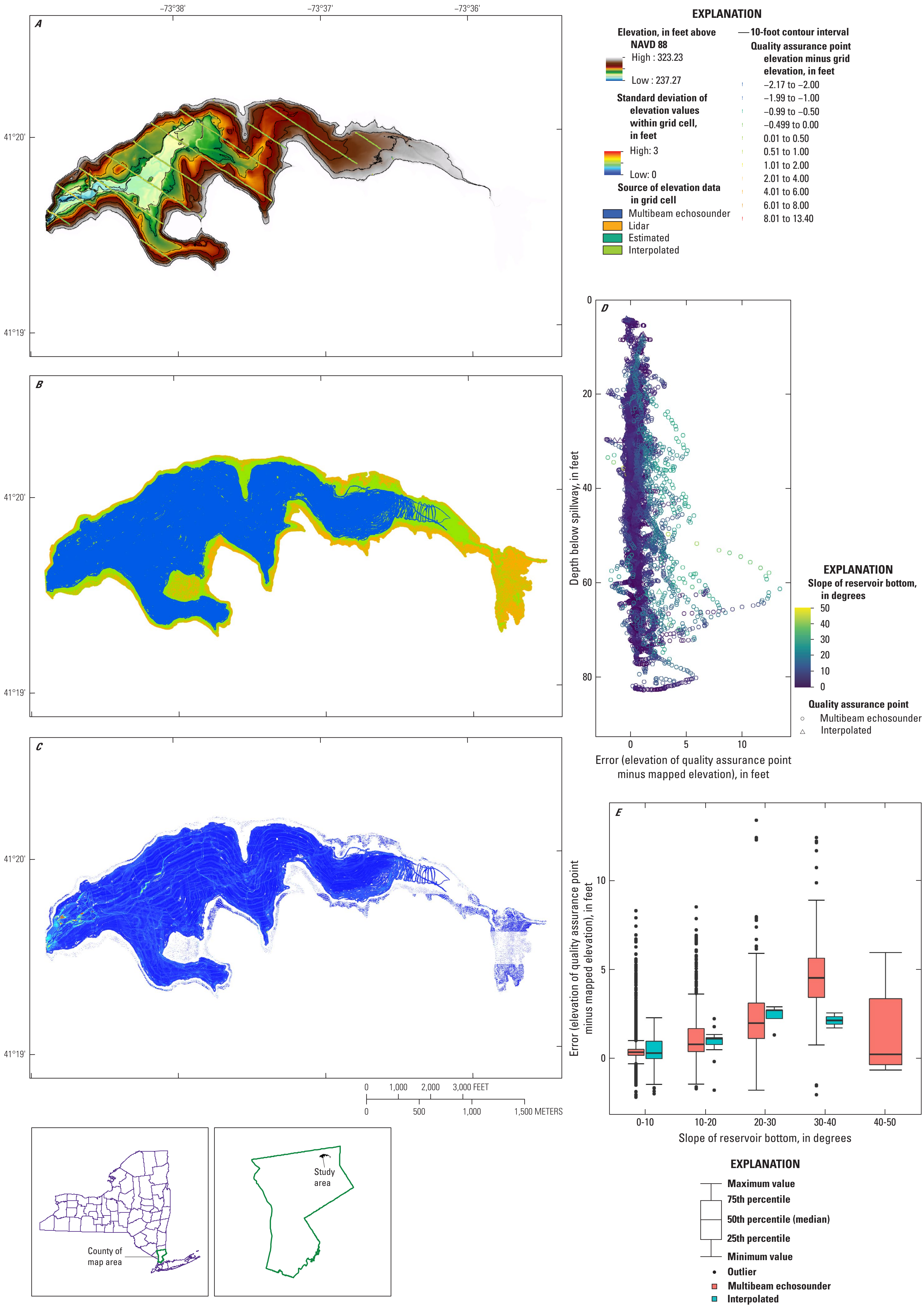

Figure 24. Results of bathymetric mapping of Titicus Reservoir in Westchester County, New York, including maps of *A*, bathymetric elevations, contours, and quality assurance points, *B*, source data type, and *C*, cell standard deviation; and plots showing comparison of quality assurance points and mapped elevation *D*, by depth and slope and *E*, by grid cell data source. Mapped data are from Nystrom and others (2021). Lidar, light detection and ranging; NAVD 88; North American Vertical Datum of 1988. A large version of this figure is available for download at https://doi.org/10.3133/sir20215057.

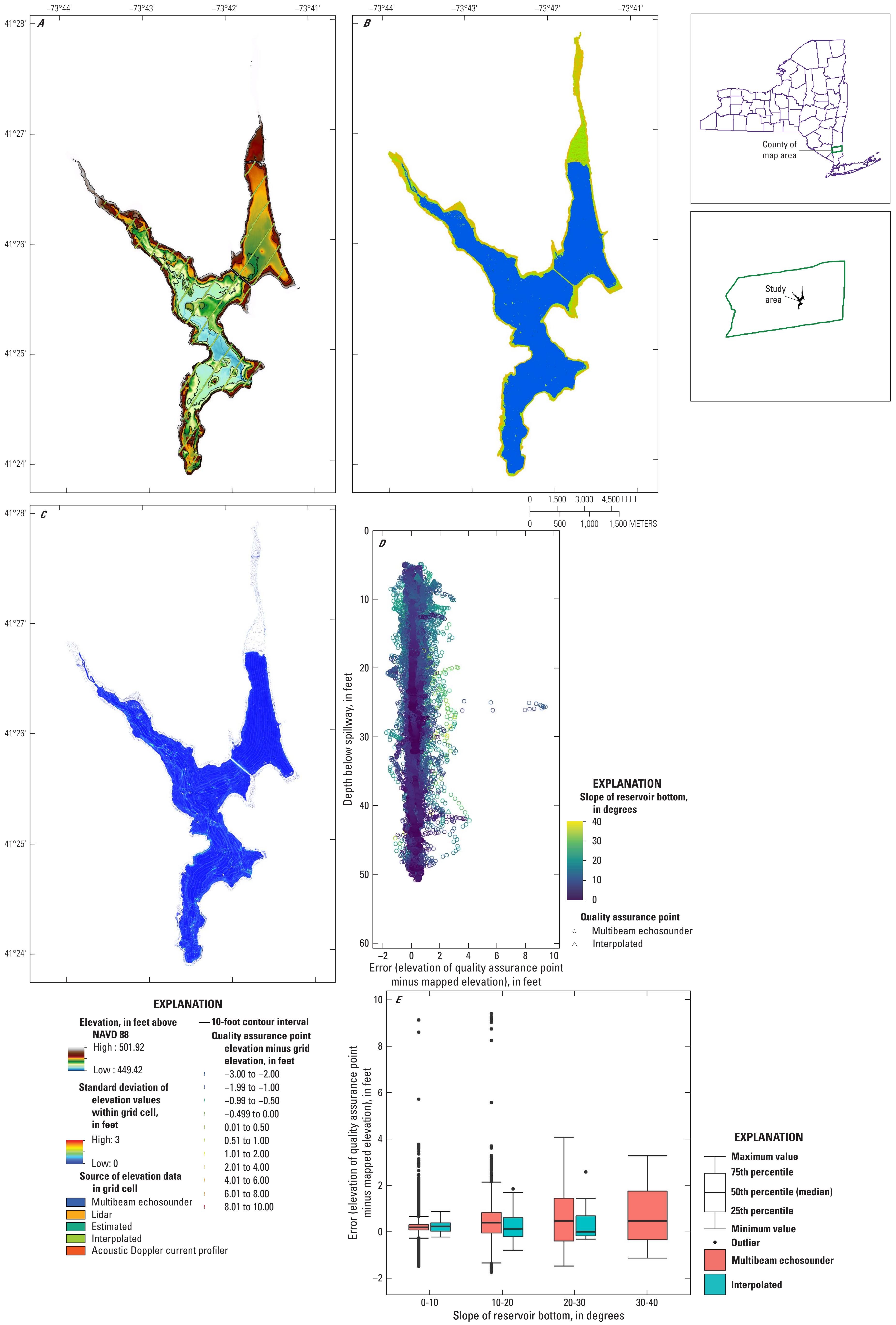

Figure 25. Results of bathymetric mapping of West Branch Reservoir in Putnam County, New York, including maps of *A*, bathymetric elevations, contours, and quality assurance points, *B*, source data type, and *C*, cell standard deviation; and plots showing comparison of quality assurance points and mapped elevation *D*, by depth and slope and *E*, by grid cell data source. Mapped data are from Nystrom and others (2021). Lidar, light detection and ranging; NAVD 88; North American Vertical Datum of 1988. A large version of this figure is available for download at https://doi.org/10.3133/sir20215057.

For more information, contact
Director, New York Water Science Center
U.S. Geological Survey
425 Jordan Road
Troy, NY 12180–8349
dc_ny@usgs.gov
or visit our website at
https://www.usgs.gov/centers/ny-water

Publishing support provided by the
Pembroke Publishing Service Center

Nystrom and others—**Bathymetry of New York City's East of Hudson Reservoirs and Controlled Lakes, 2017 to 2019**—SIR 2021–5057

ISSN 2328-0328 (online)
https://doi.org/10.3133/sir20215057